Science with IRAM-NOEMA

Jérôme PETY
(IRAM & Obs. de Paris)

Obs. de Paris, Sep. 19th, 2014

Comet Hartley 2 with the Plateau de Bure Interferometer

Boissier et al. 2014, Icarus, 228, 197

-Maps+time variations (nucleus complex rotation):
Gas production mainly from the nucleus small lobe
-OnOff/Interferometric flux ratio:
Significant outgassing from icy grains

Full agreement with simultaneous fly by observations

Deep Impact observations (4 Nov.) :
Gas jets (letf) and snowballs (right) around the nucleus

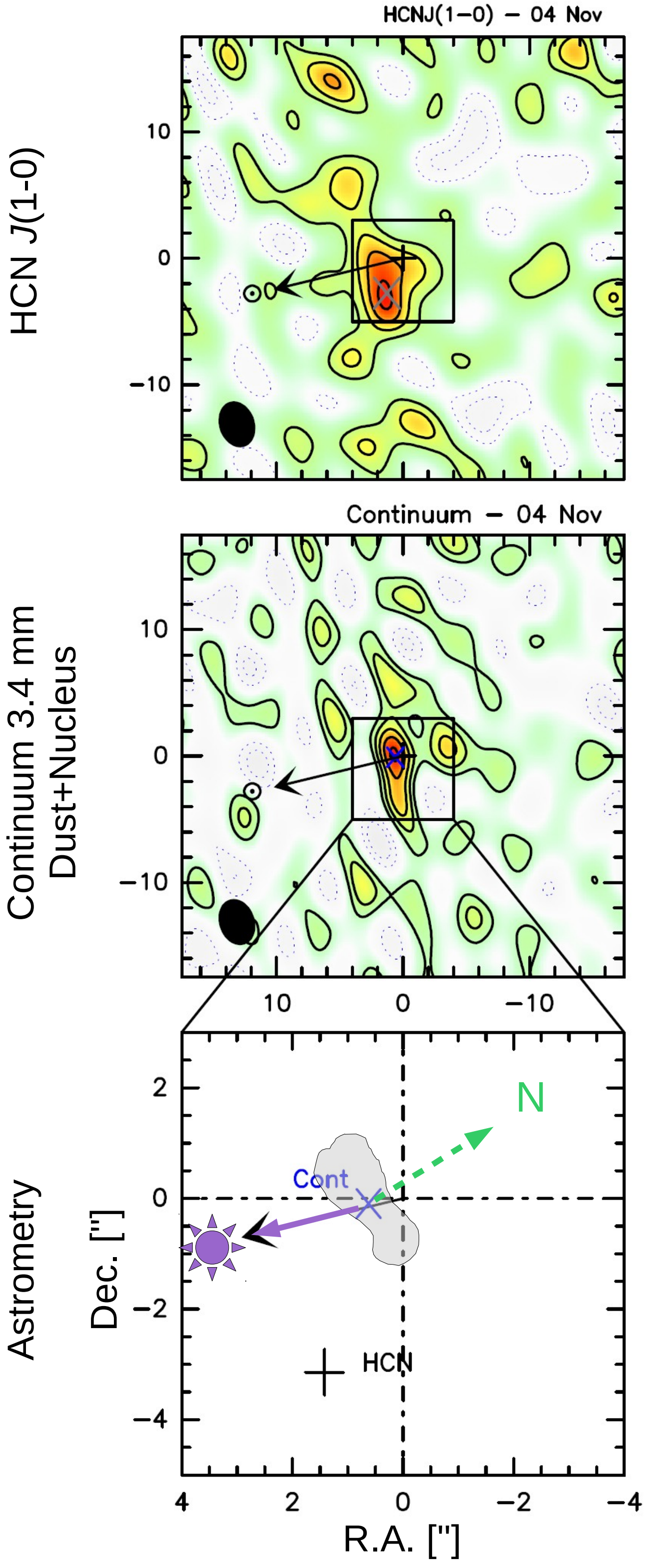

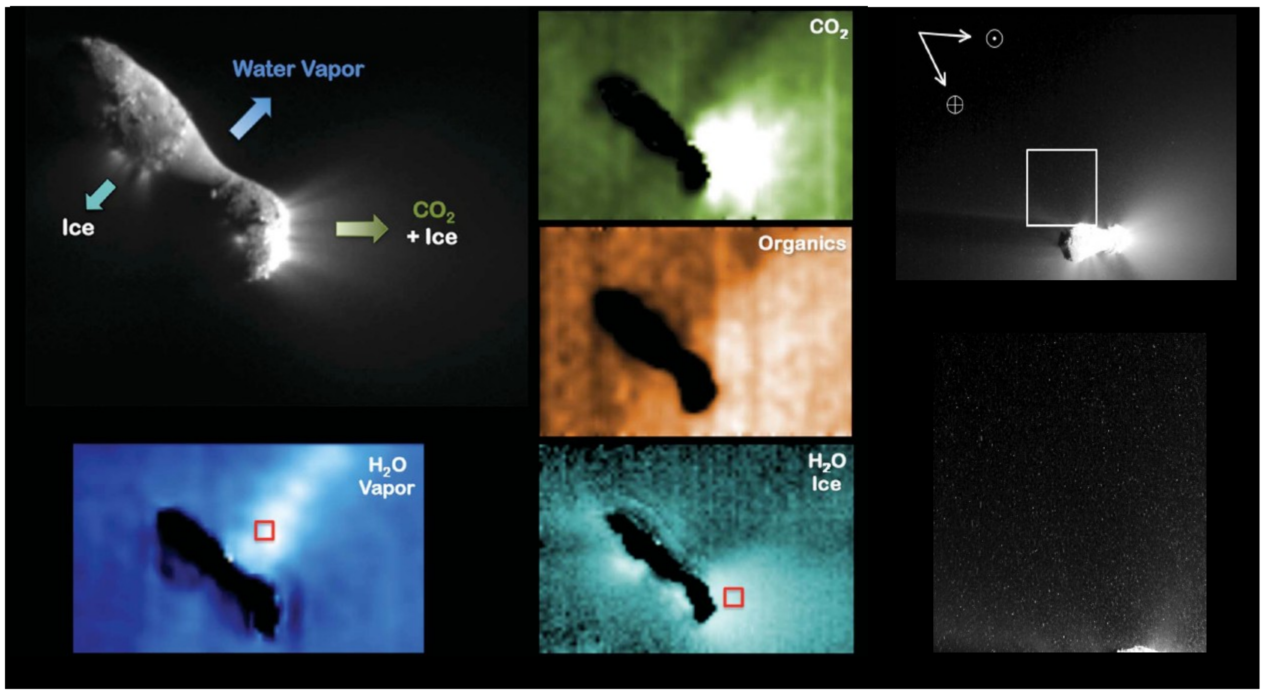

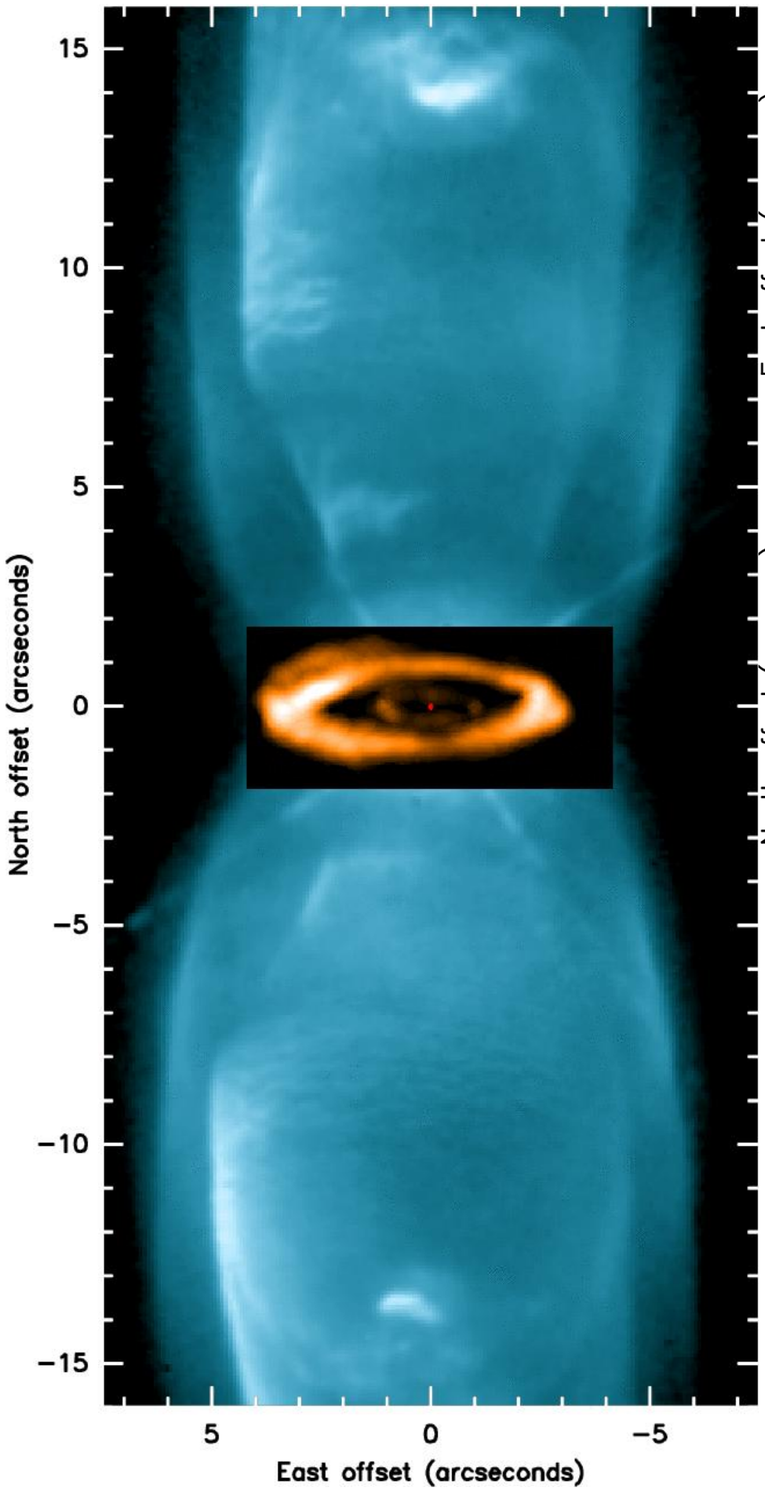

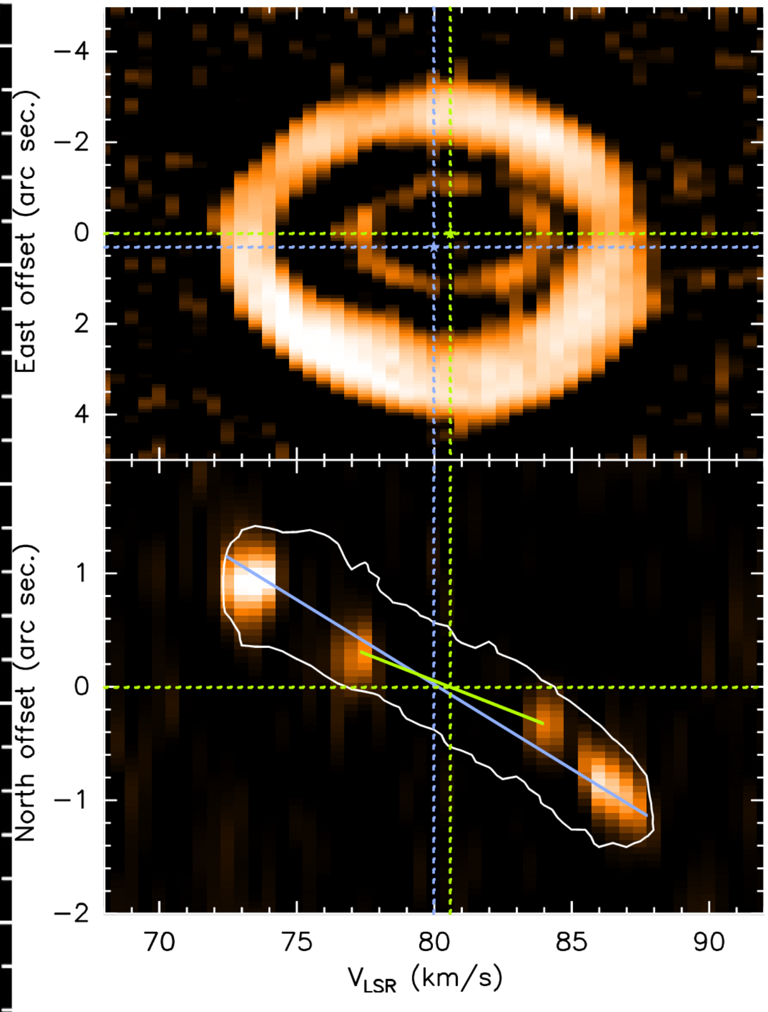

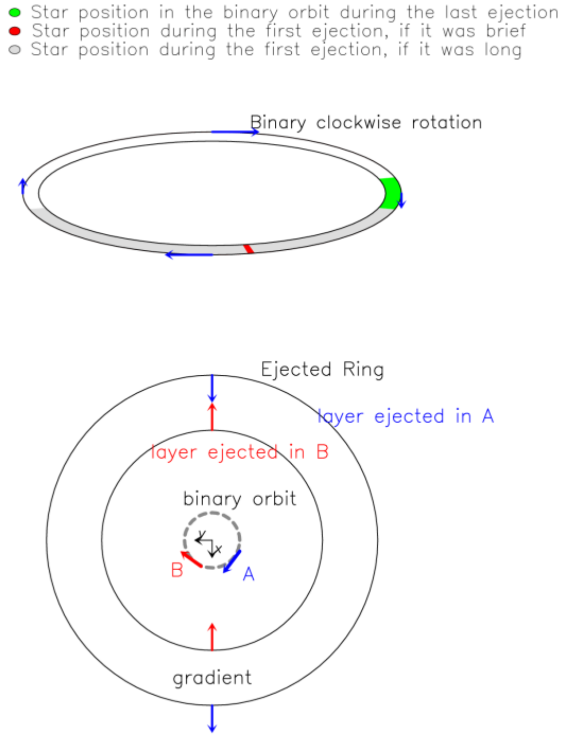

M 2-9 CO *J*=2-1

The analysis of the spatio-kinematics of the two detected equatorial ring-like outflows allow probing the central binary system (Castro-Carrizo et al, 2012)

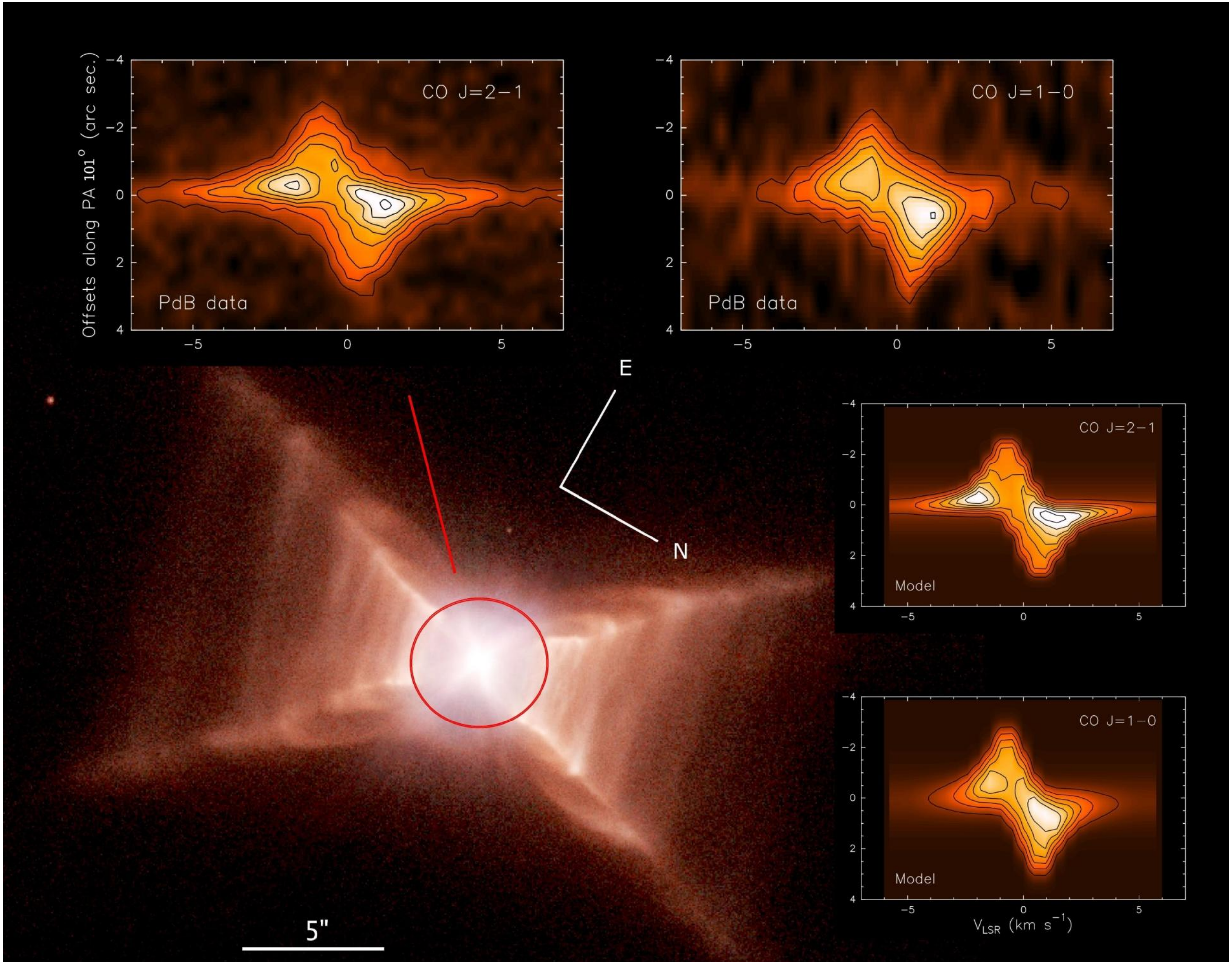

The Red Rectangle the only rotated disc probed so far… (Bujarrabal et al 2005, 2013)

$0.4''$-imaging of 9 faint ($< 30\,$mJy) Class-II disk
⇒Small ($< 15\,$AU), high surface density disks (Piétu et al. 2014)

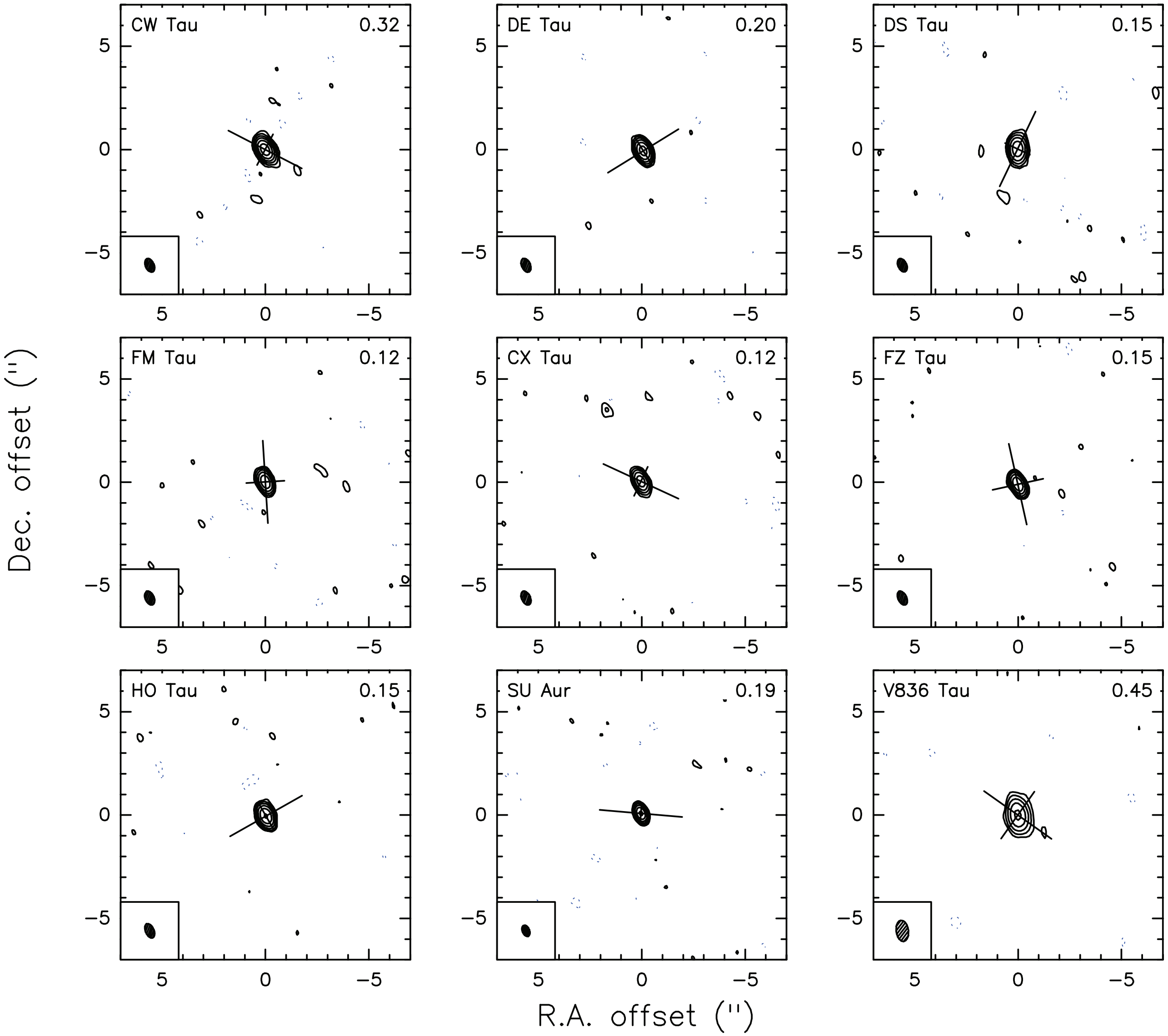

Up to 25% of the disk population in Taurus
Potential link with compact planetary systems found by the Kepler mission?

The Horsehead WHISPER line survey (PI: Pety, Guzmán, Gratier et al.)

Wideband High-resolution Iram-30m Surveys at two Positions with Emir Receivers

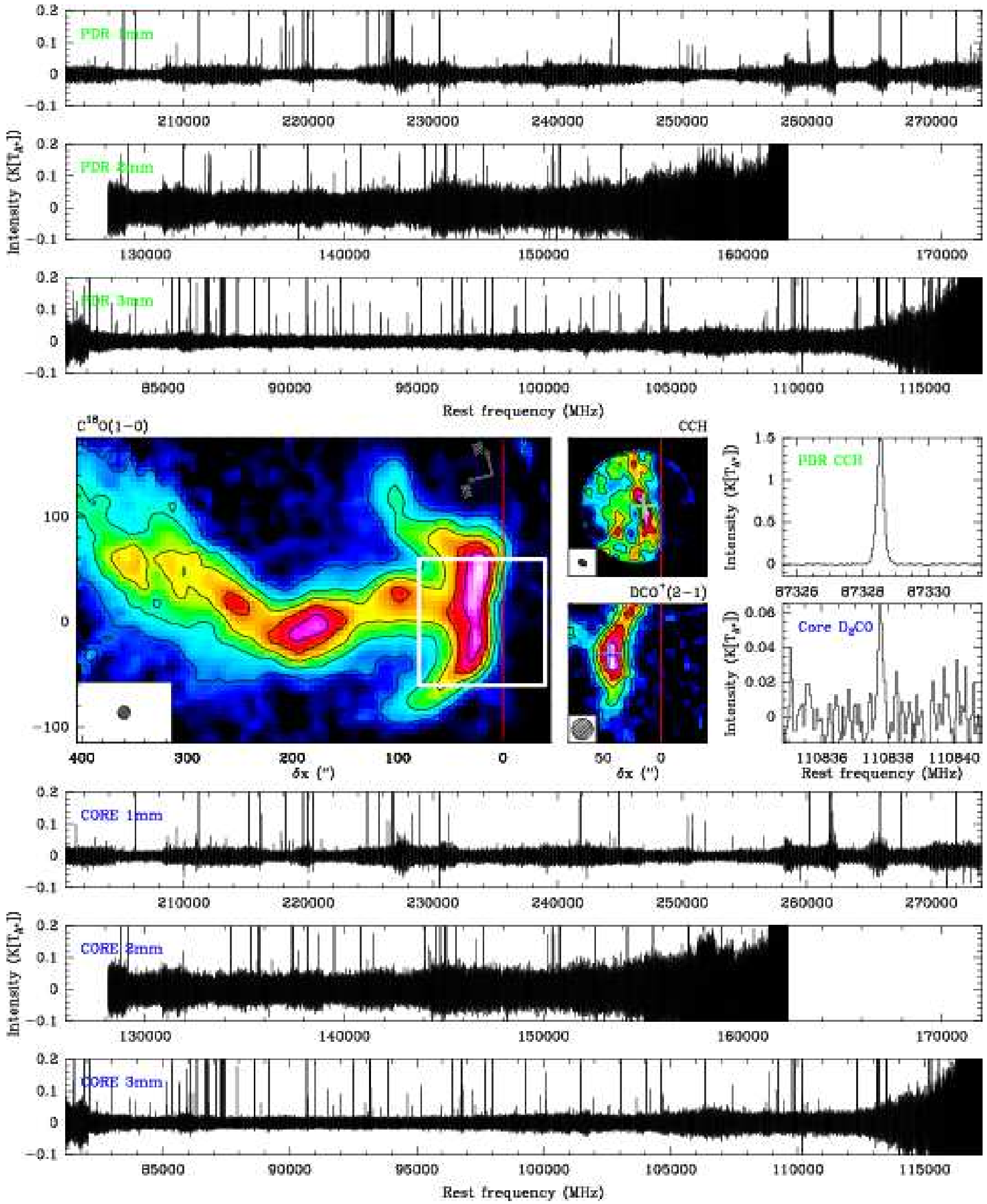

IRAM-30m telescope

$\sim$ 75 hours per position

	1 mm	2 mm	3 mm
Bandwidth	73 GHz	34 GHz	36 GHz
Resolution	195 kHz	49 kHz	49 kHz
Sensitivity	8.6 mK	18.5 mK	8.1 mK

- 2 positions observed
  $\Rightarrow$ Detailed comparison of the chemistry of UV-illuminated and UV-shielded gas
- 30 species (plus their isotopologues) are detected with up to 7 atoms

CF^+ emission in the Horsehead

Guzmán et al. 2012a

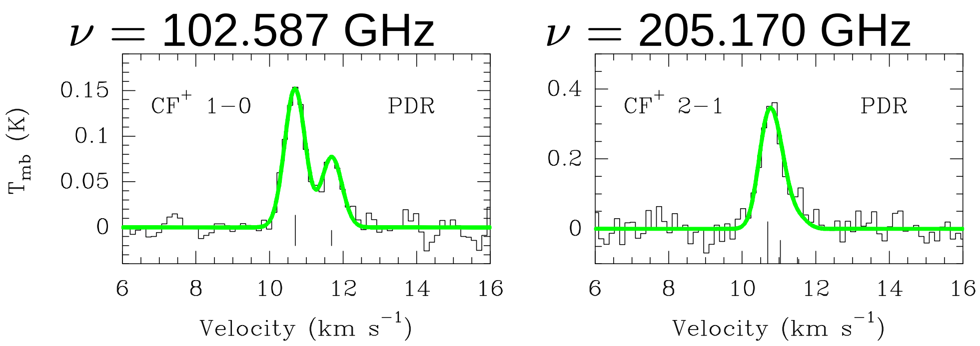

- Simple chemistry:

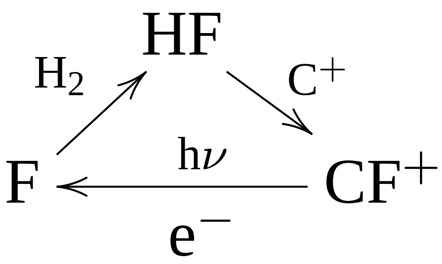

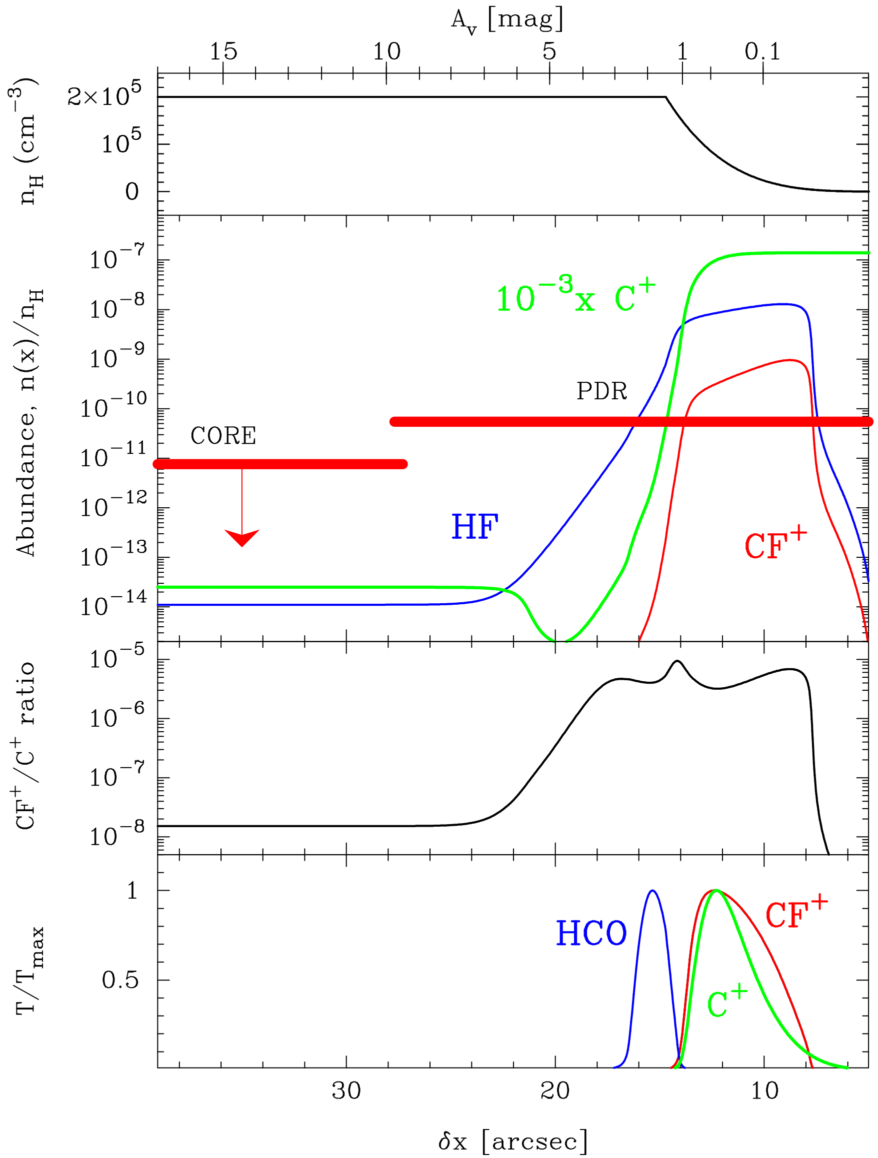

Significant overlap between CF^+ and C^+

CF^+ as a proxy of C^+ and a measure of [F]

So?

C^+: Herschel (12″), SOFIA (15″)

CF^+ can be used as a tracer of C^+ associated to molecular gas that can be observed from the ground

- Simple chemistry:

$$N(CF^+) \propto [F]$$
$$F/H \simeq (0.6 - 1.5) \times 10^{-8}$$

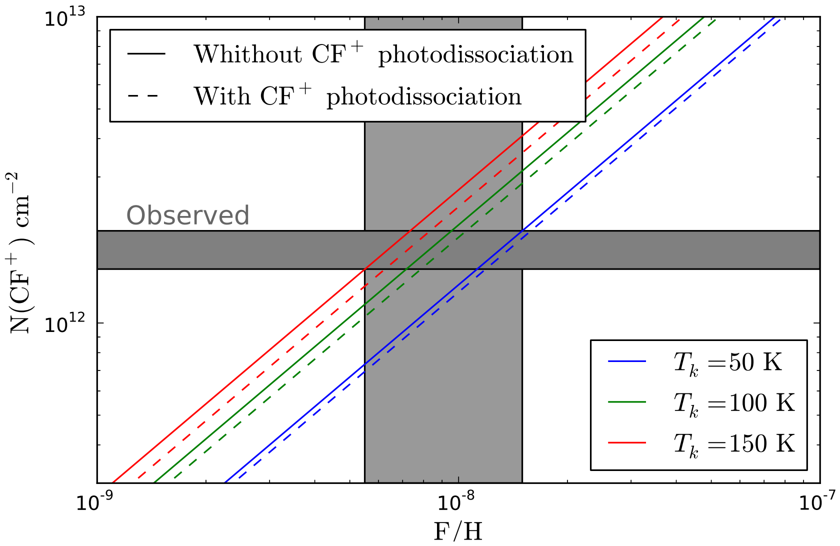

Guzmán et al. 2012a

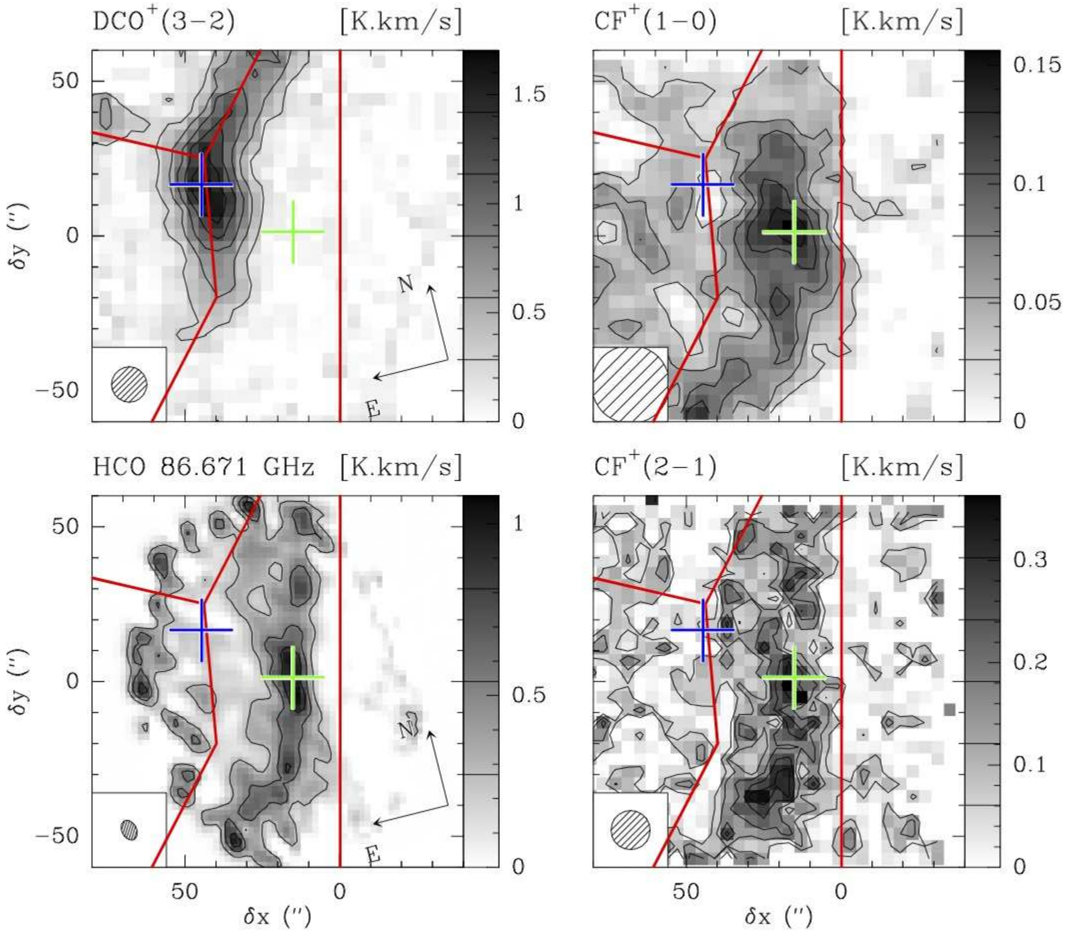

CF^+ emission arises from the UV-illuminated edge

A new species in the ISM: Tentatively attributed to C_3H^+

Pety et al. 2012

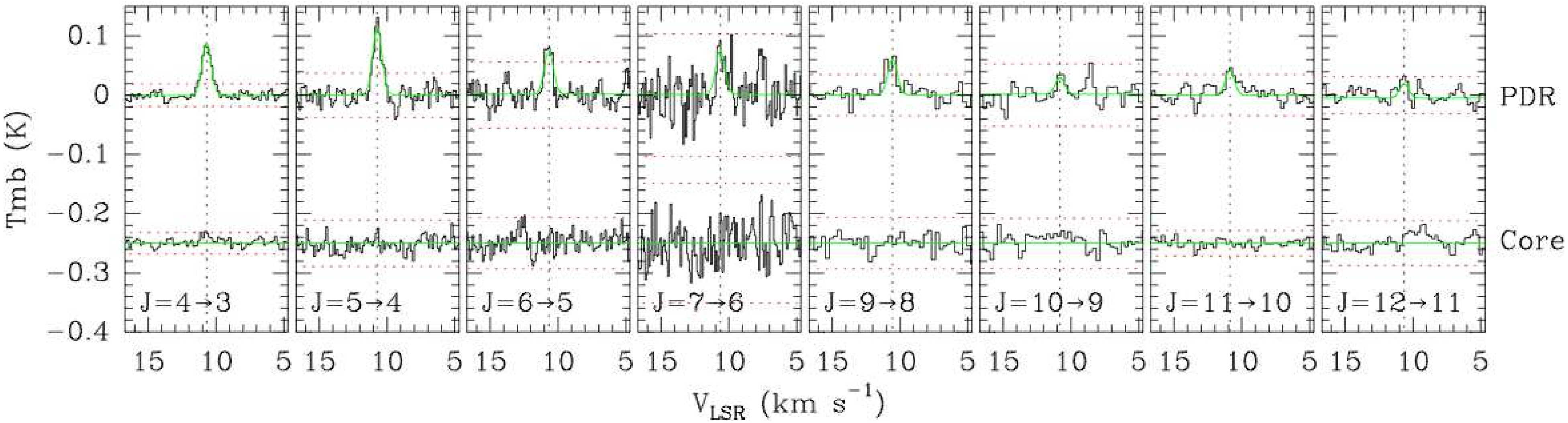

- Consistent set of 8 unidentified lines towards the PDR position.
- Linear rotor, with a $^1\Sigma$ electronic ground state.
- The deduced rotational constant is close to that of $l-C_3H$.
- Reactive molecule with a spatial distribution similar to small hydrocarbon chains.

$\Rightarrow$ Most probable candidate: C_3H^+

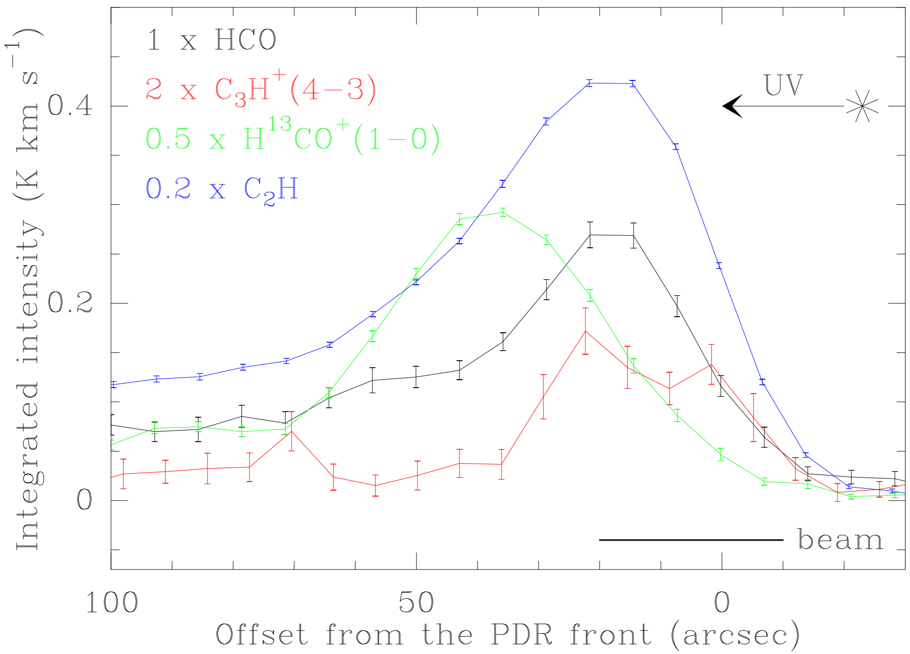

Formation of the small hydrocarbons: Top-Down chemistry

Pety et al. 2012

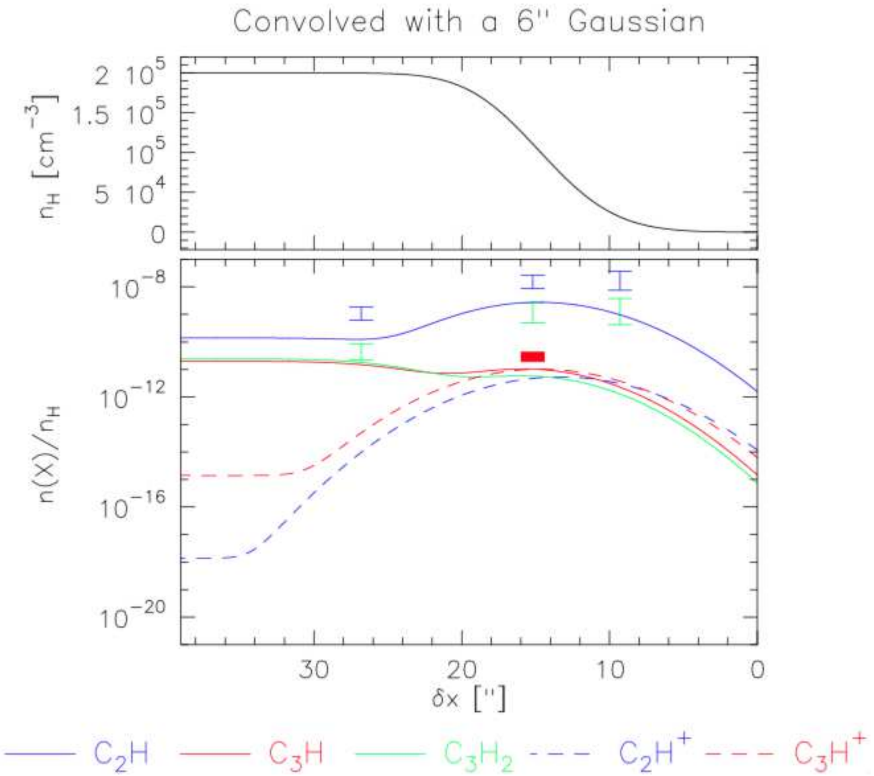

$$C_2H_2 \xrightarrow{C^+} C_3H^+ \xrightarrow{H_2} C_3H_2^+ \xrightarrow{e^-} C_3H$$

$$C_3H^+ \xrightarrow{H_2} C_3H_3^+ \xrightarrow{e^-} C_3H_2$$

- $[C_3H^+] = 2 \pm 0.7 \times 10^{-11}$
  Consistent with gas-phase model
- $[C_2H]$ and $[C_3H_2]$ are 1-2 orders of magnitude higher than in models
- Good correlation between PAH and hydrocarbons emission

UV-field fragments PAHs and small grains into small hydrocarbons

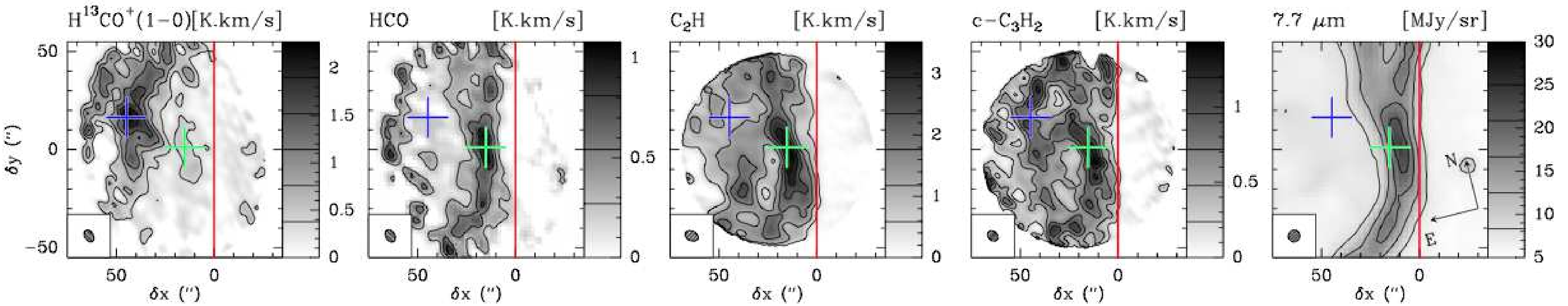

Complex molecules: Grain surface chemistry

Thermal desorption

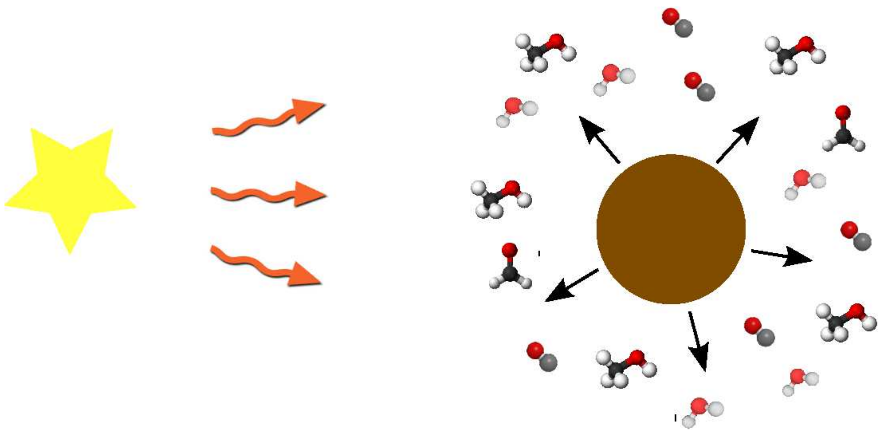

- Hot cores
- Hot corino
- High UV illuminated PDRs
- $T_{\mathrm{sublimation}} \simeq 40$ K (H_2CO)
- $T_{\mathrm{sublimation}} \simeq 80$ K (CH_3OH)

Photo-desorption

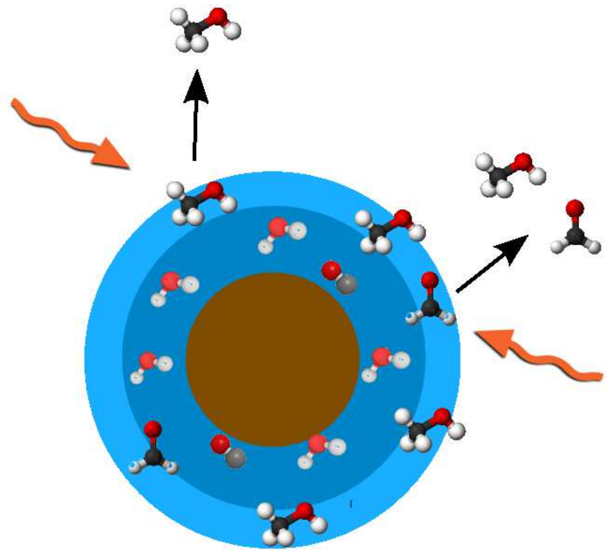

- UV-shielded dense cores (secondary photons)
- Low UV illuminated PDRs

In the Horsehead $T_{\mathrm{dust}} \simeq 20 - 30$ K

$\rightarrow$ Clean environment to isolate the role of photodesorption.

Gas-phase vs. Grain surface chemistry

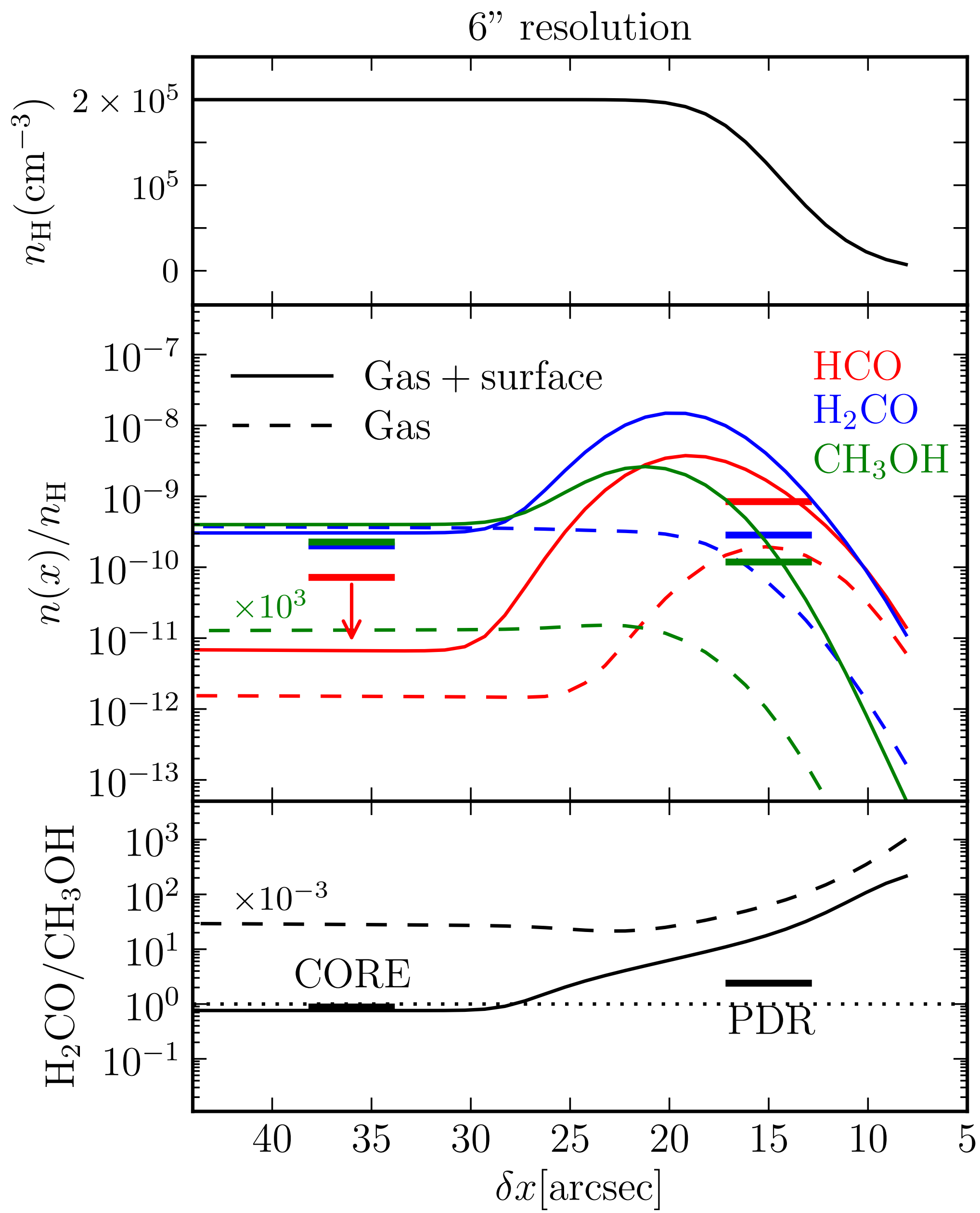

Guzmán et al. 2013

PDR models: Meudon PDR Code

Evelyne Roueff

Le Petit et al. (2006)

Le Bourlot et al. (2012)

- Pure gas-phase
  H_2CO: CORE ✓, PDR ✗
  CH_3OH: CORE: ✗, PDR ✗
- Gas-phase + grain surface

⇒ Photo-desorption is needed to explain the observed H_2CO and CH_3OH abundance in the PDR.

High-angular resolution (6″) PdBI maps

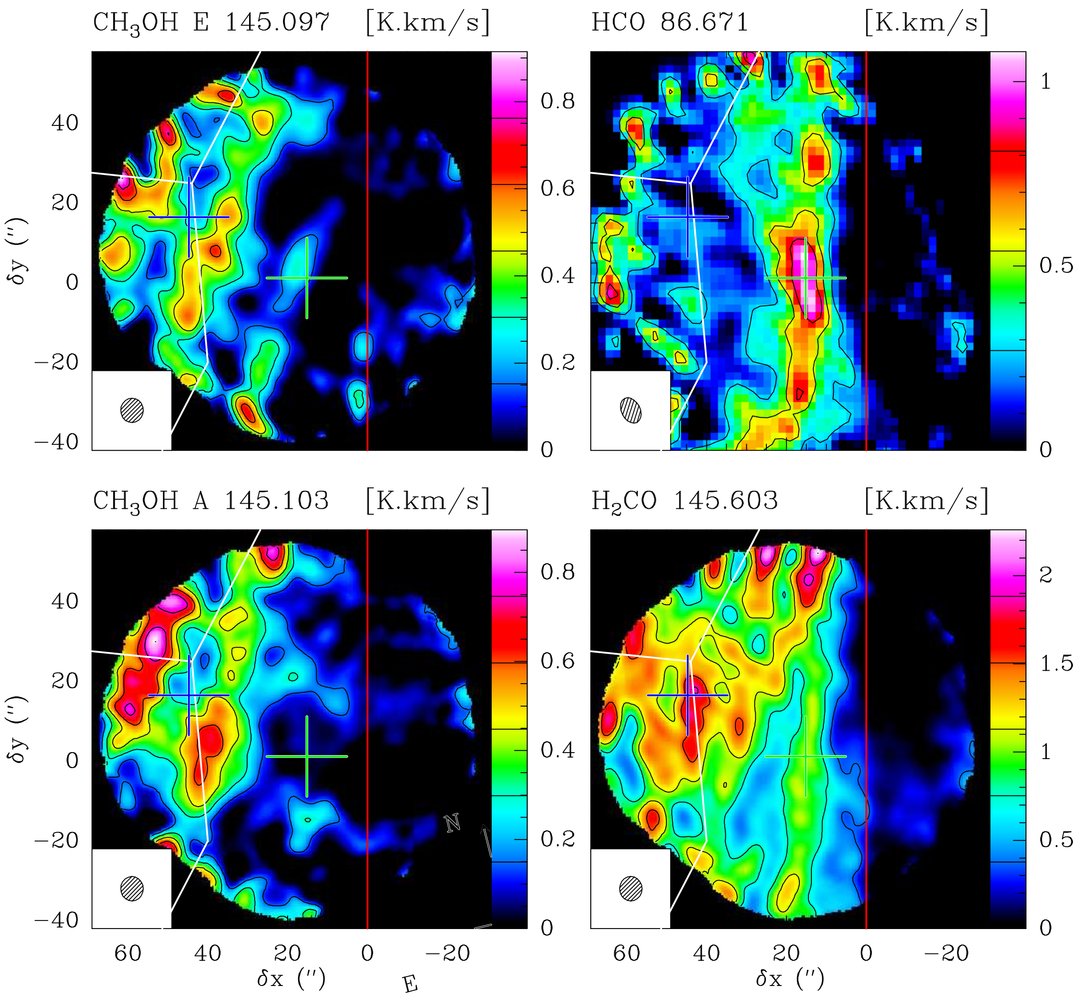

Guzmán et al. 2013

Different H_2CO formation mechanism?

PDR: grain surface
Dense core: gas-phase

Evidence:

- Different ortho-to-para ratio (2 in the PDR, 3 in the core)
- Spatial distribution $\rightarrow$ CH_3OH depletion at core
- Radiative transfer analysis of CH_3OH yields lower gas density at core
- Pure gas-phase model can reproduce H_2CO abundance at the dense core

CH_3OH**:**
$\rightarrow$ **envelope around dense core**
H_2CO**:**
$\rightarrow$ **envelope and dense core itself**

Nitriles in the Horsehead: CH_3CN and HC_3N

Gratier et al. 2013

HC_3N

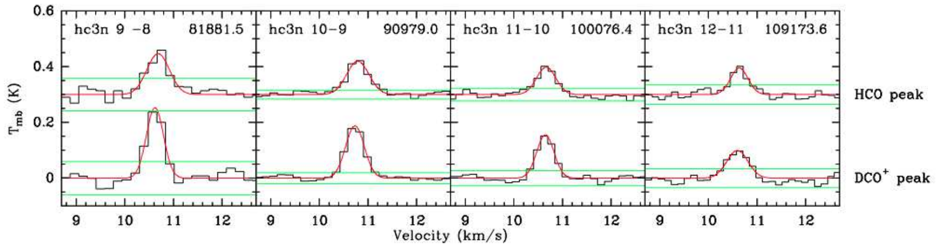

CH_3CN

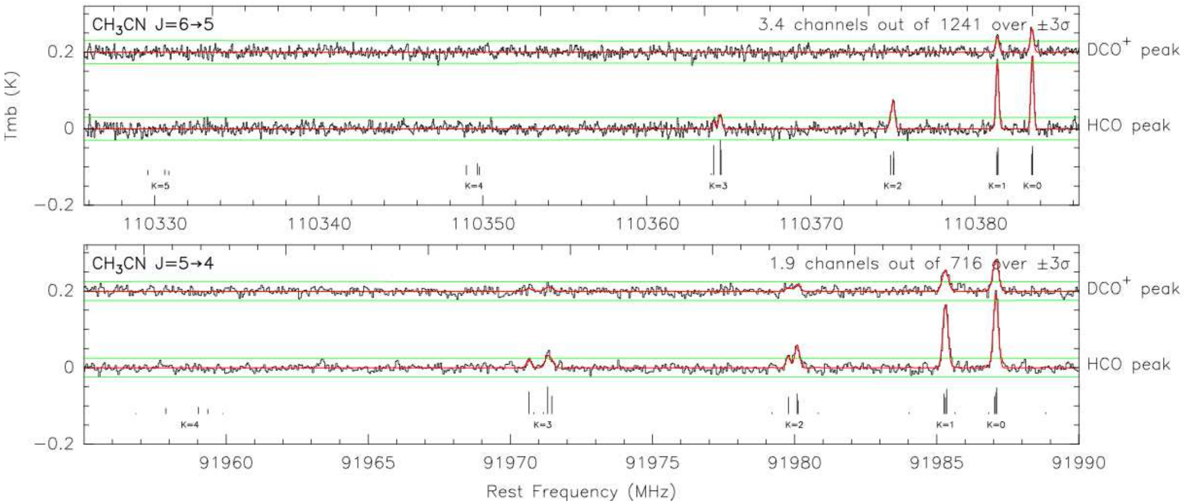

HC_3N

- $[HC_3N]_{PDR} \simeq [HC_3N]_{Core}$

CH_3CN

- $[CH_3CN]_{PDR} \simeq 2.5 \times 10^{-10}$
- $[CH_3CN]_{PDR} \simeq 30\ [CH_3CN]_{Core}$

$\longrightarrow$ Different chemistry

Gas-phase model predicts CH_3CN abundance $\sim$ 2400 times lower

$\longrightarrow$ **Enhanced abundance due to FUV field?**

- Enhanced abundance of precursors in the PDR
- UV photo-processing of N bearing ices ($C_2H_5NH_2$) followed by photodesorption (Danger et al. 2011)

The anatomy of a Giant Molecular Cloud: Orion B

PI: J.Pety, P.Gratier, V.Guzman, P.Tremblin S.Bardeau, M.Gerin, J.Goicoechea, F.LePetit, H.Liszt, R.Lucas, K.Oberg, N.Peretto, E.Roueff, and A.Sievers

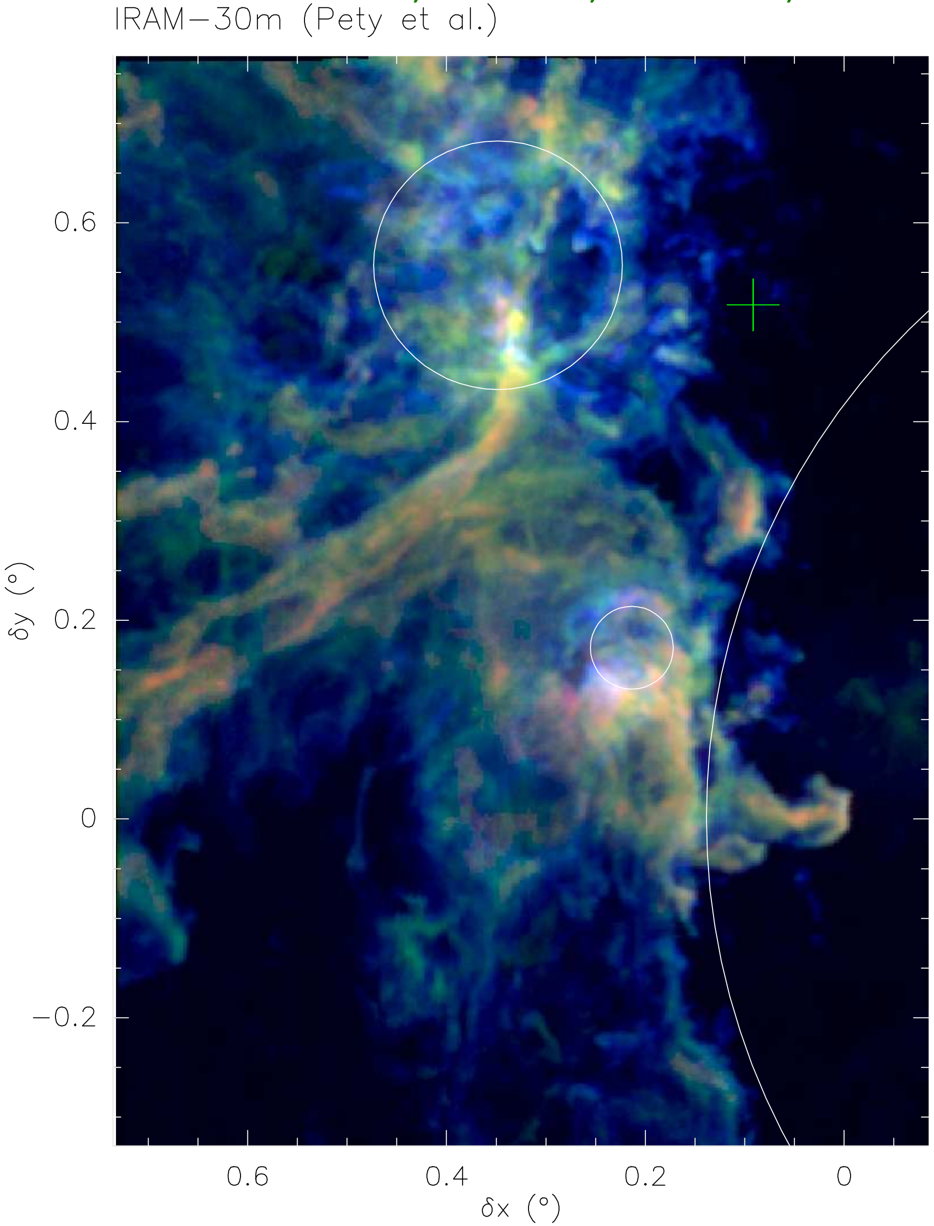

$C^{18}O$ (J=1–0), ^{13}CO (J=1–0), ^{12}CO (J=1–0)

Integration time 124 hours (42 hours in Aug. 2013, 24 hours in winter 2014, 58 hours in Aug. 2014).

Field of view $0.81 \times 1.10°$, *i.e.*, 0.9 square degree.

Observing mode Position switched On-The-Fly (mostly a single coverage).

Spatial resolution From $22.5''$ to $30.5''$, *i.e.* Nyquist sampling $\Rightarrow$ images of 315×420 pixels.

Bandwidth 32 GHz (2 tunings) from 84 to 116 GHz.

Spectral resolution 200 kHz resolution, *i.e.*, $0.5 - 0.7\,\mathrm{km\,s^{-1}}$.

Number of channels $\Rightarrow$160 000 channels, *i.e.*, at 24 images per seconds, it makes a movies of 1h50!

Field of view $\times$ channels 144 000 channel x square degree (*i.e.*, the equivalent of twice of the sky in 5 days!).

Median noise level 0.1 to 0.5 K (T_{mb}).

A sea of noise Clear signal detected in $\sim$ 800 channels, or 0.5% of the data (a video of about 30 seconds).

Data size 900 GB of raw data.

PAWS ID card (http://www.mpia.de/PAWS)

E. Schinnerer (PI), A. Hughes, S. Meidt, D. Colombo, J.Pety, A. Leroy
S. Garcia-Burillo, G. Dumas, K. Schuster, C.Kramer, C. Dobbs, T. Thompson

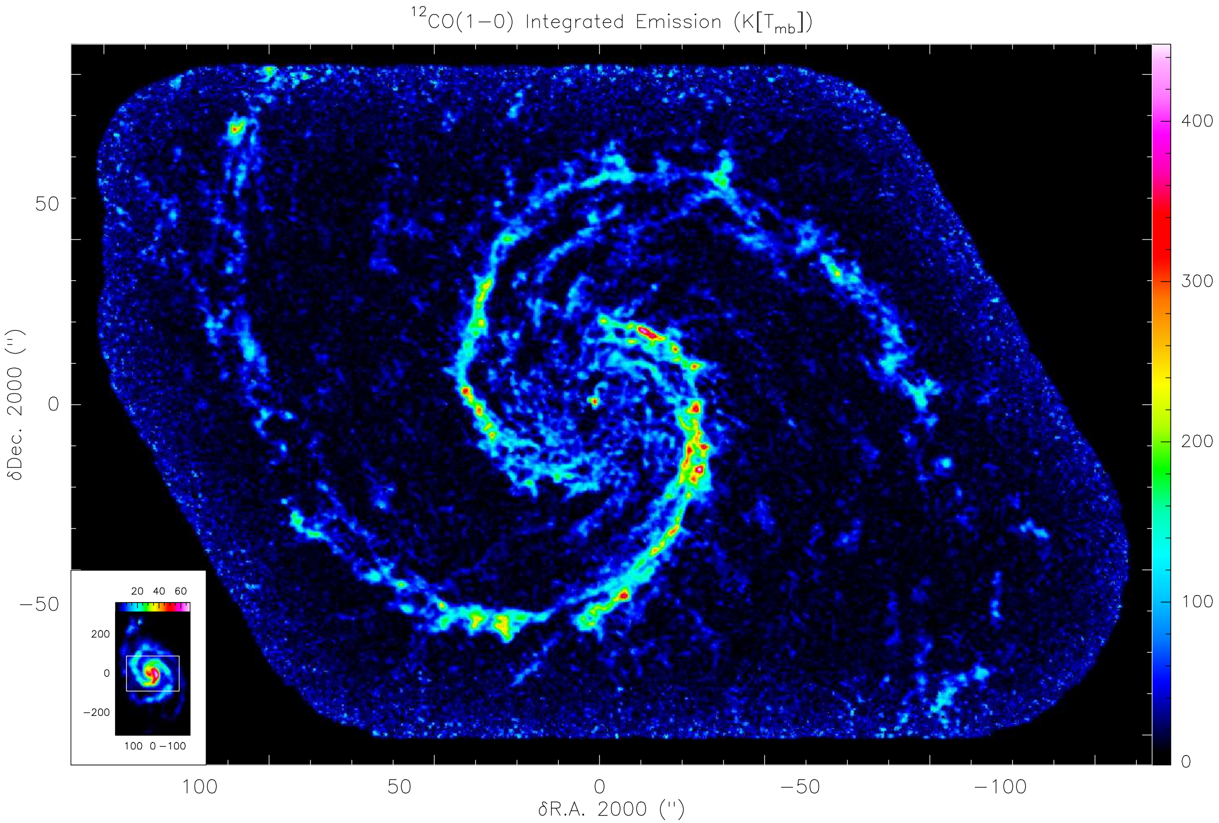

Observations and data reduction:

- Mosaic of 60 fields at 3 mm, *i.e.*, ^{12}CO (J=1–0).
- 170 hours of PdBI time + 40 hours of IRAM 30m time.
- On-source time: 8 hr in D, 15 hr in C, 43 hr in B and 60 hr in A configuration
  $\Rightarrow$ 454 000 visibilities $\times$ 1024 channels.
- Imaging and deconvolution require images of 2 Mpixels (in fine: only 36 000 fully independant pixels).
  $\Rightarrow$ 40 hours to deconvolve 120 channels (up to 320 000 components per channel).

Facts

Distance 7.6 ± 1 Mpc.
Inclination $21 \pm 3°$.
Position angle $173 \pm 3°$.
Field of view $270'' \times 170''$ or 10×6 kpc.
Final resolution $\sim 1.1''$ or ~ 40 pc

Sensibility $\sim 0.4\,\mathrm{K}[T_{\mathrm{mb}}]$ in $5\,\mathrm{km\,s^{-1}}$
Total CO luminosity $1.4 \times 10^9\,\mathrm{K\,km\,s^{-1}\,pc^2}$
Total molecular mass $6.2 \times 10^9\,\mathrm{M_\odot}$
Mean brightness $7.6\,\mathrm{K\,km\,s^{-1}}$
Mean mass surface density $33\,\mathrm{M_\odot\,pc^2}$

Why/How HD TV changes your life

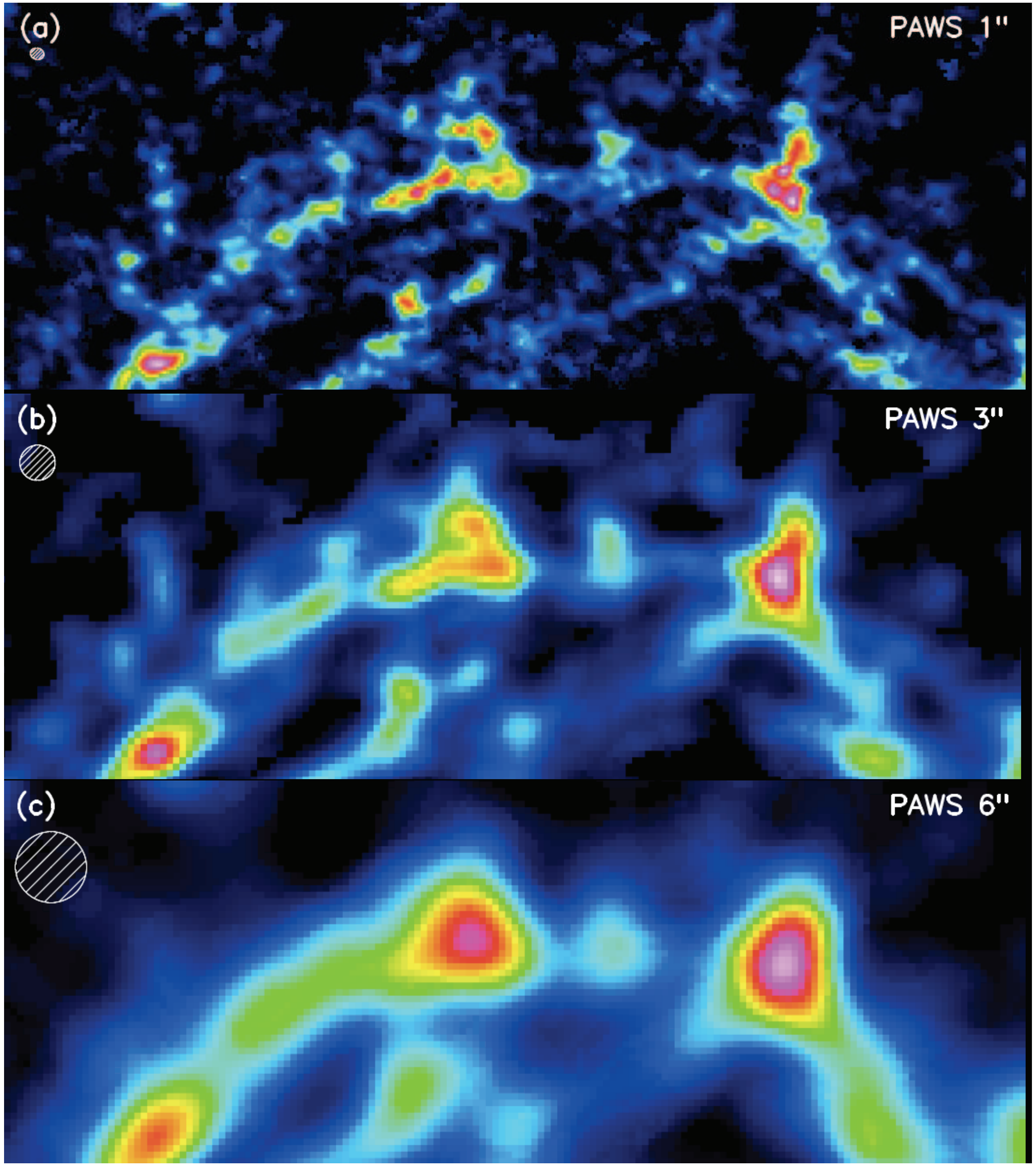

$M_{\mathbf{H}_2} = 4 \times 10^9\,\mathrm{M}_\odot$ in PAWS FoV using the standard X_{CO} factor (Pety et al. 2013)

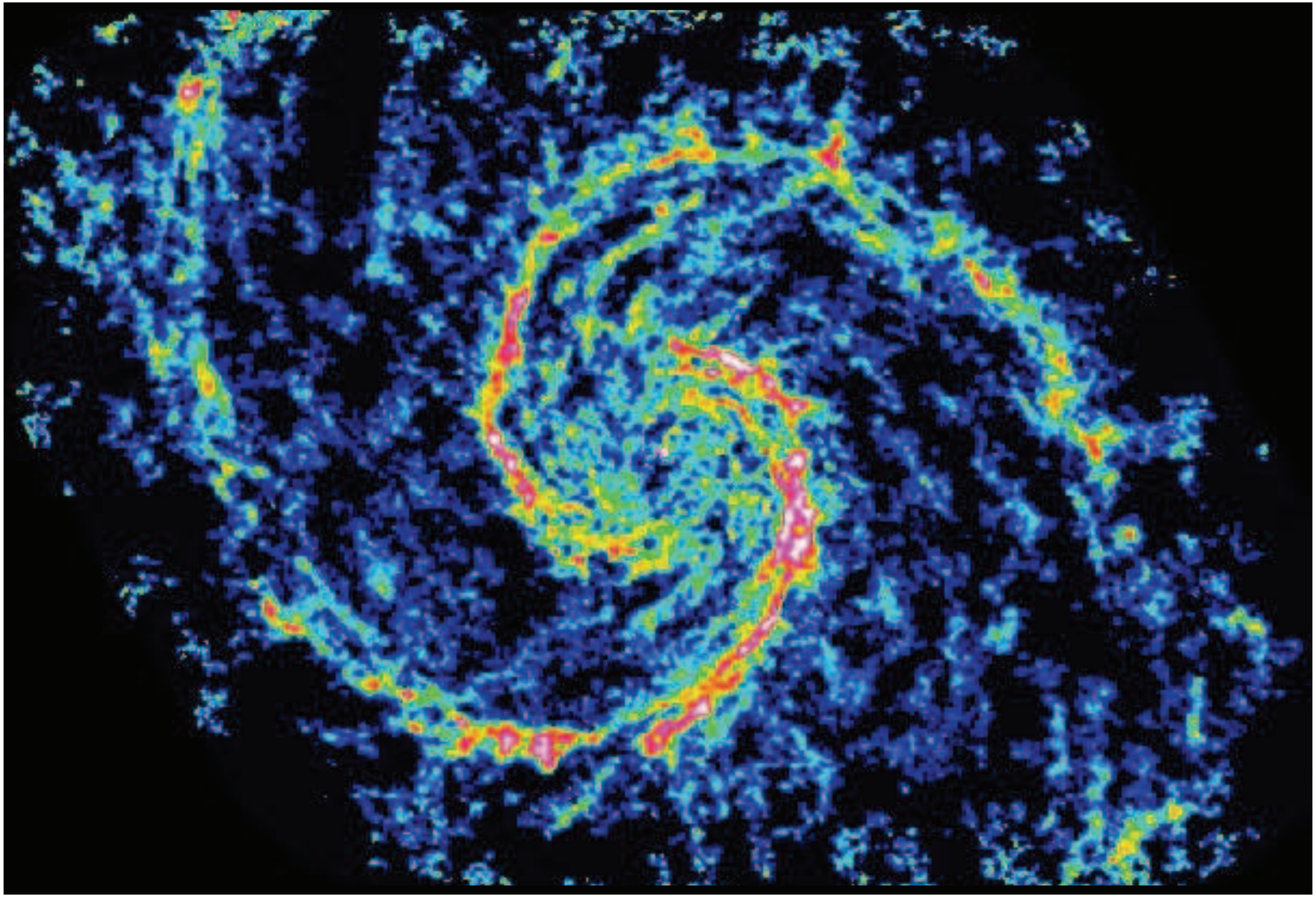

55% of the total CO flux can be attributed to 1,500 GMCs
(Colombo et al. 2014a)

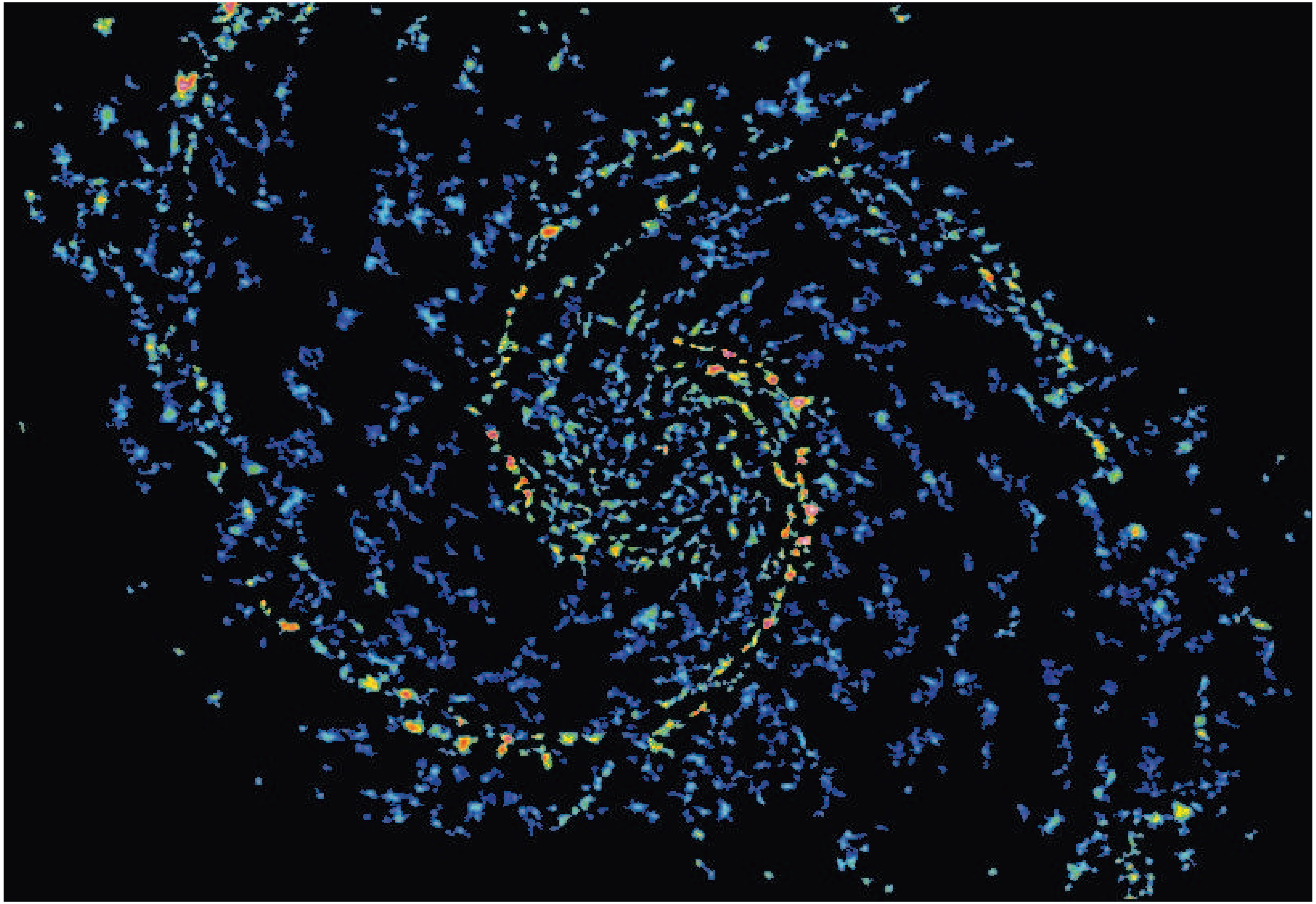

⇒ Where is the rest?

A CO diffuse thick disk in M51:
$\sim$ 50% of the flux is resolved
at scales $\geq 36'' \sim 1.3$ kpc
(Pety et al., 2013)

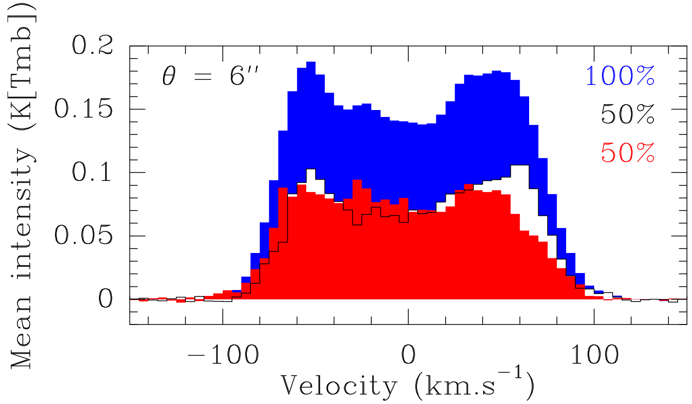

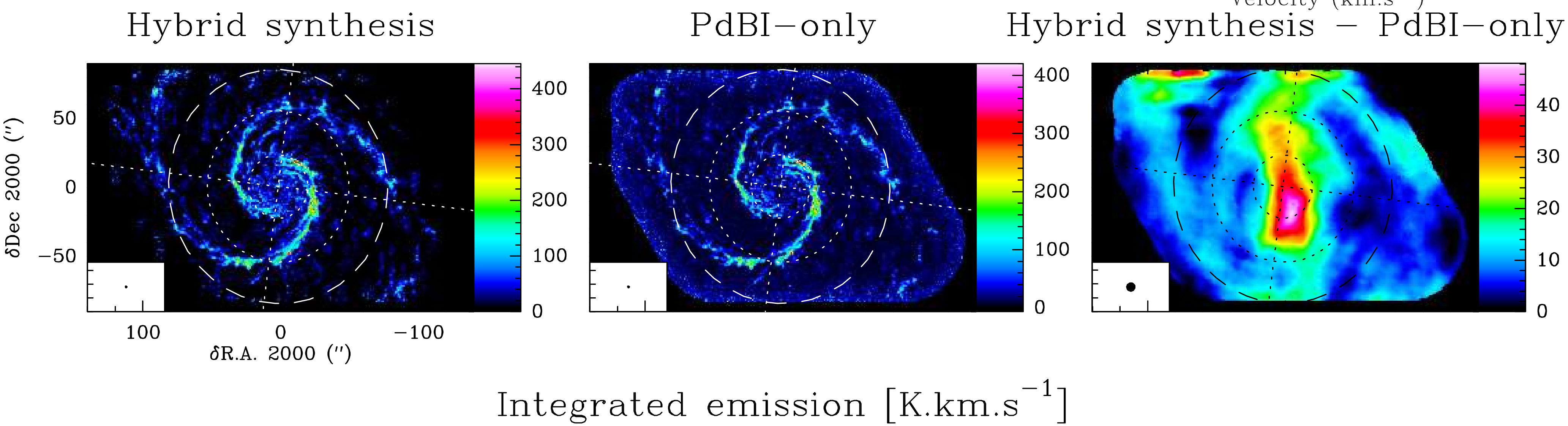

PdBI-only component

Bright From 2 to 16 K with a median of 2.5 K.

Compact It fills only $\sim$ 2% of the surface.

Filtered component

Faint From 0.07 to 1.36 K with a median of 0.14 K.

Extended It fills $\sim$ 30% of the surface.

A CO diffuse thick disk in M51:
A dense and diffuse components of very different vertical scale heights, which probably mix in the galactic plane.
(Pety et al., 2013)

Relative linewidths

Fact The filtered component has a velocity dispersion at least twice as large as the compact component.

Interpretation (using Koyama & Ostriker 2009) The extended component has a Gaussian scale height ($\sim 200\,\text{pc}$) typically 5 times as large as the compact component one ($\sim 40\,\text{pc}$). The Galaxy scale height is 57 pc (Ferriere 2001, Cox 2005).

Consequence The extended component average density ($1\text{H}_2\ \text{cm}^{-3}$) is one order of magnitude lower than the compact component one ($10\text{H}_2\ \text{cm}^{-3}$). The Galaxy average density is $0.29\text{H}_2\ \text{cm}^{-3}$ (Ferriere 2001, Cox 2005).

$P_{\rm int} \sim P_{\rm ext} \Rightarrow$ Clouds must "know" about their environment
(Hughes et al. 2013b)

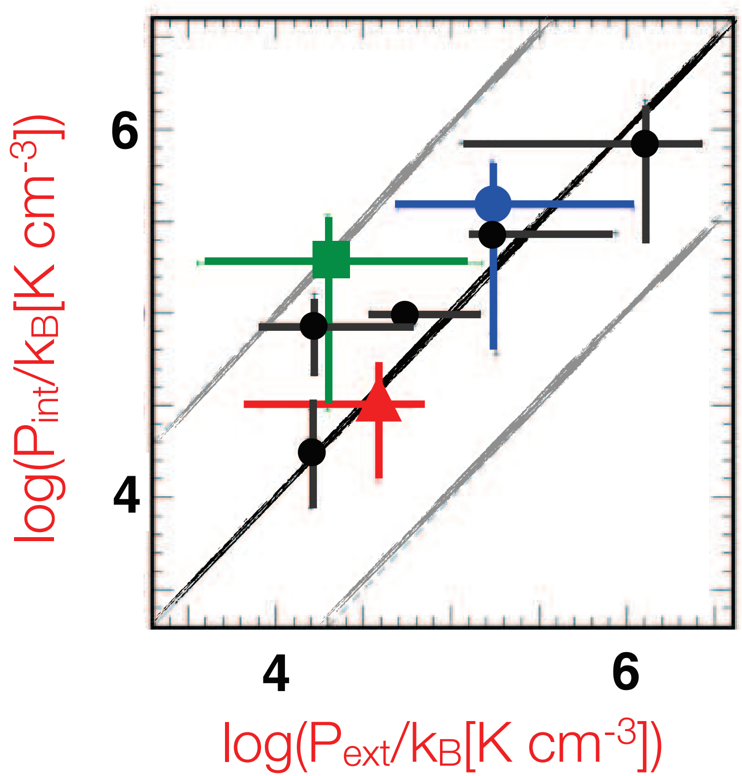

- M51
- M33
- LMC
- NGC 6946, M64, NGC 4449, NGC 2976, NGC 4214

Multi-wavelength comparison: I. ^{12}CO (J=1–0) (Schinnerer et al. 2013)

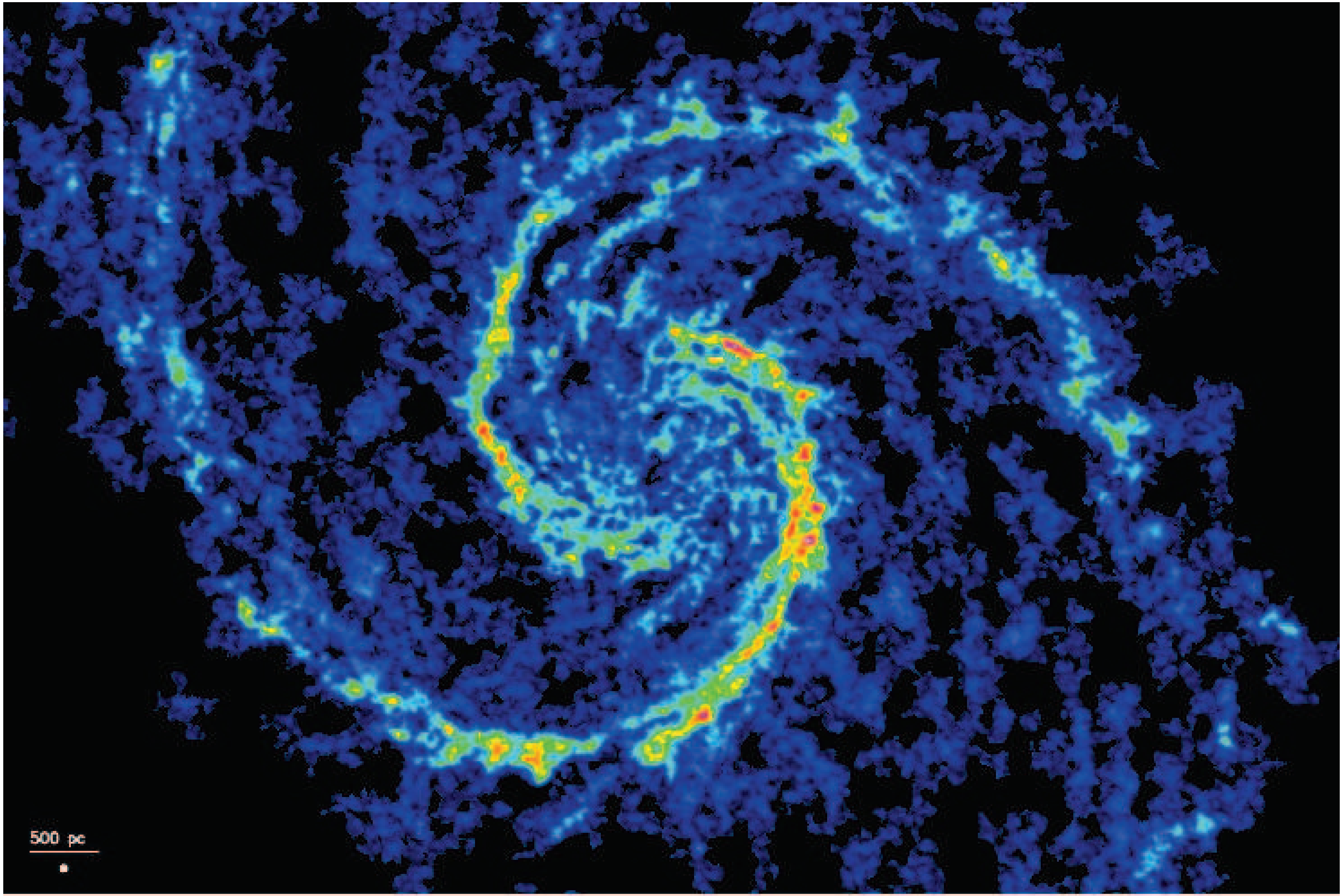

Multi-wavelength comparison: II. HST I-H (Cold dust reddening) (Schinnerer et al. 2013)

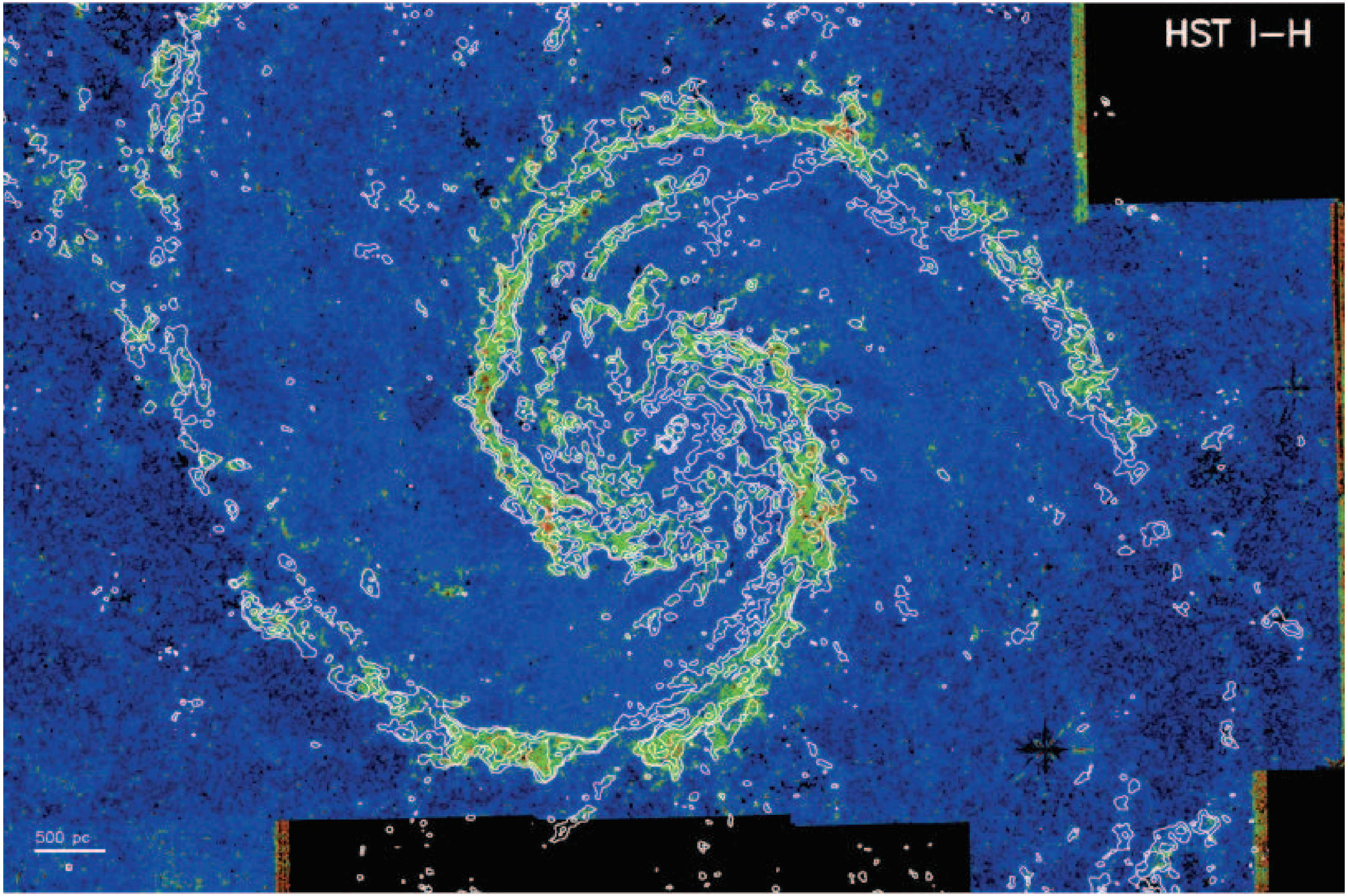

Multi-wavelength comparison: III. PACS 70 μm (Hot dust) (Schinnerer et al. 2013)

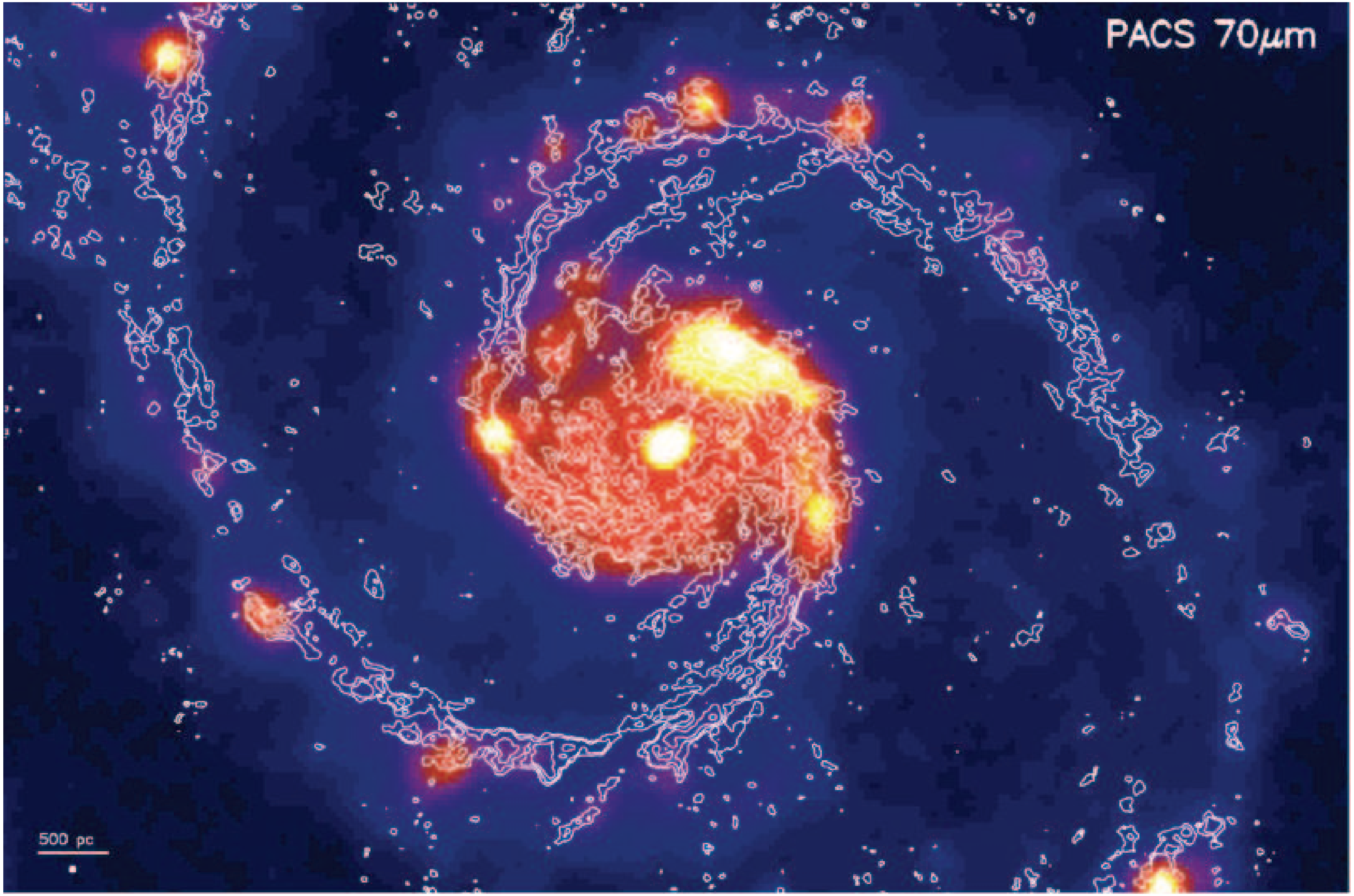

Multi-wavelength comparison: IV. HST Hα (HII regions ⇒ OB stars) (Schinnerer et al. 2013)

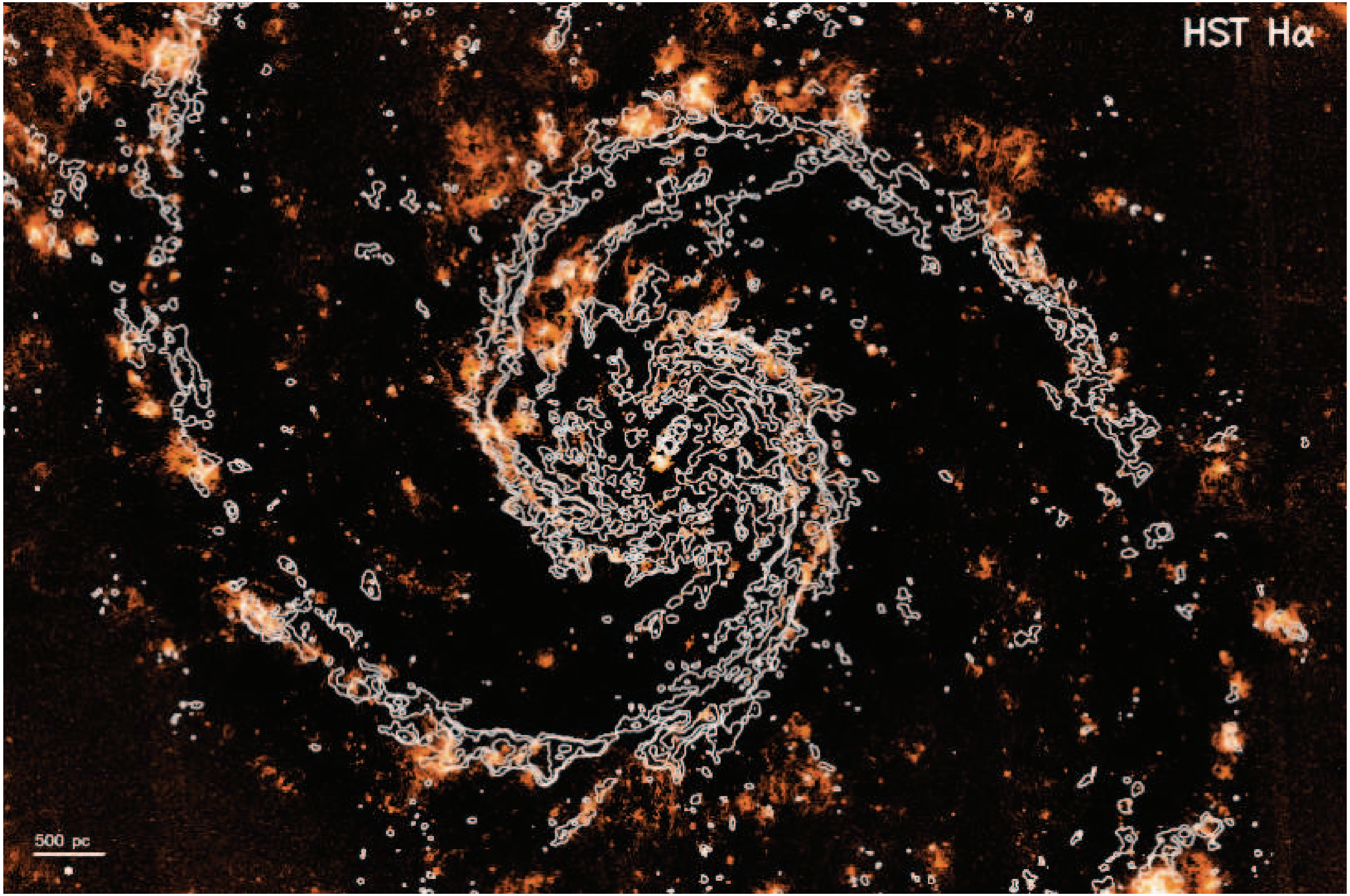

Multi-wavelength comparison:
V. Galex FUV (Stars younger than 100 Myr) (Schinnerer et al. 2013)

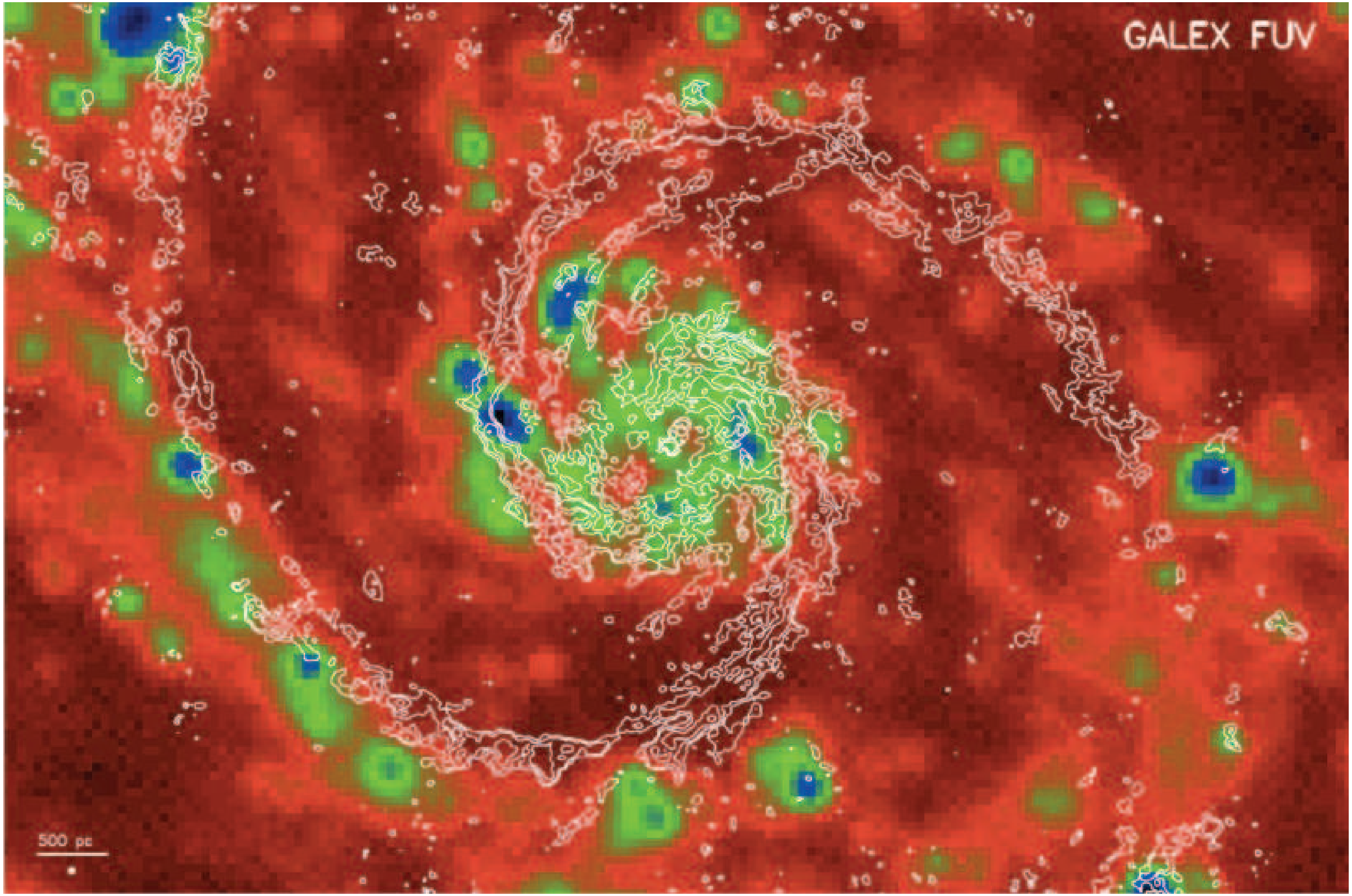

Multi-wavelength comparison (Schinnerer et al. 2013)

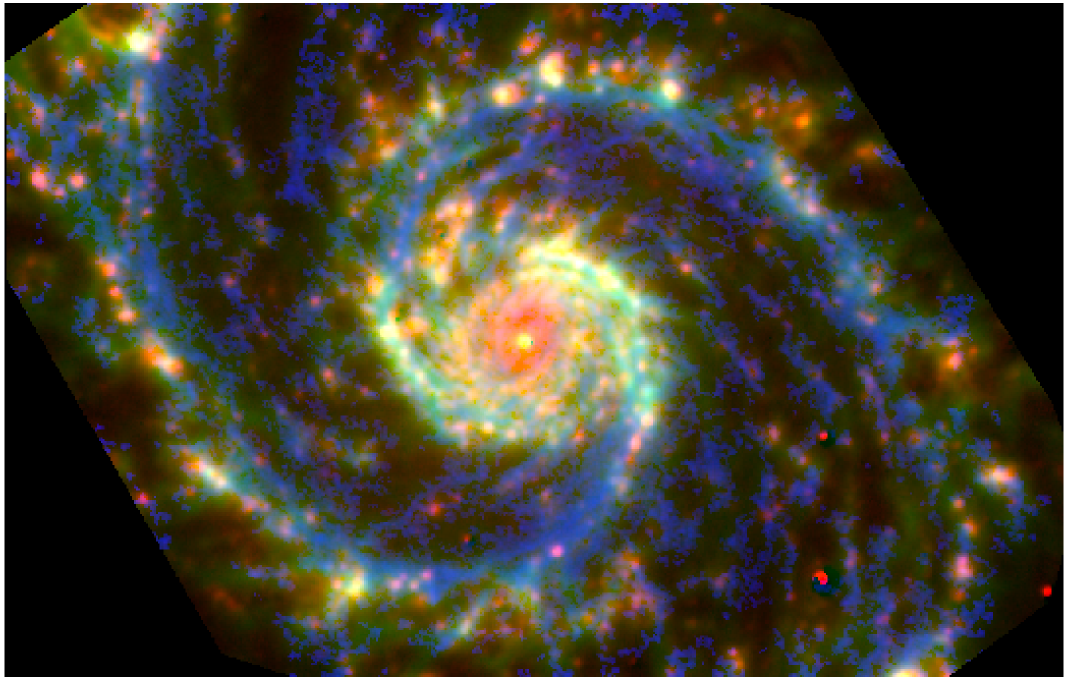

SINGS Hα Spitzer 8 μm ^{12}CO (J=1–0)

Molecular ring Coincident star formation

Spiral arm, inside spiral corotation Suppressed star formation.

Spiral arm, outside spiral corotation Offset star formation.

Streaming increases gas depletion time (Meidt et al. 2013)

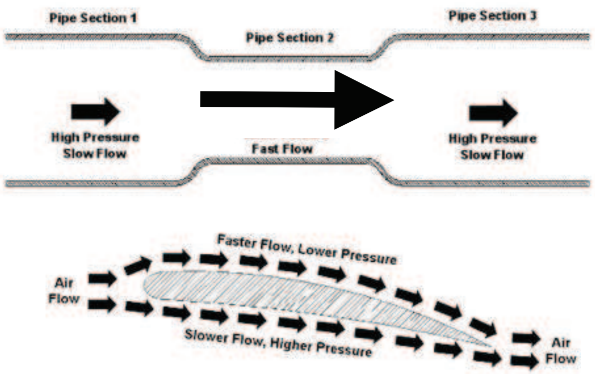

- $P_{\mathrm{int}} \sim P_{\mathrm{ext}} \Rightarrow$ Surface pressure is relevant.
- Larger streaming motions (Hughes et al. 2013).
  $\Rightarrow$ Reduced surface pressure.
  $\Rightarrow$ Increase the mass threshold for gravitational collapse.
  $\Rightarrow$ Reduced % of gravitationally unstable clouds.
  $\Rightarrow$ Lower star formation efficiency.

$0.3''$-imaging of C^+ at $z = 5.2$
$\Rightarrow$ HDF850.1 is a merger (Neri et al. 2014)

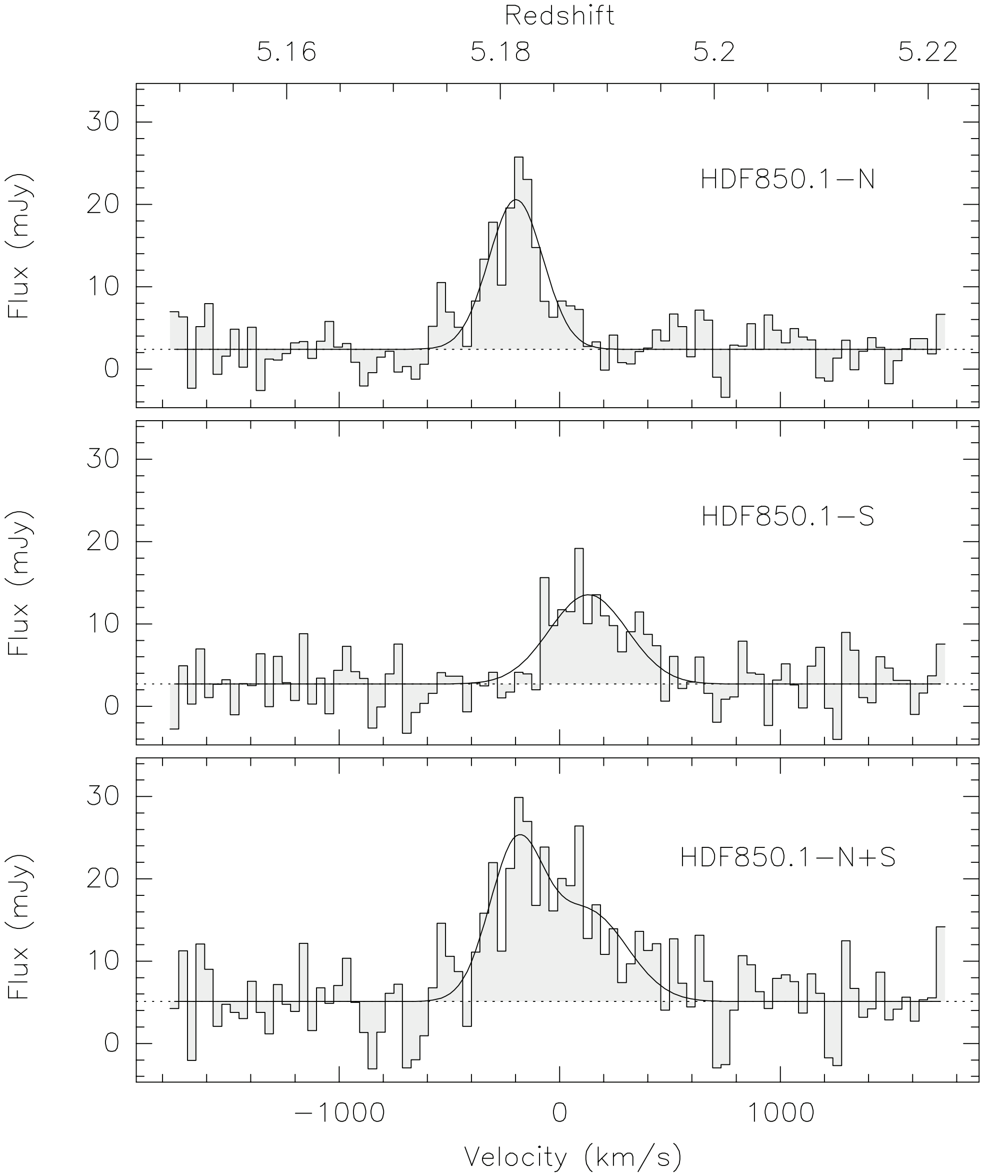

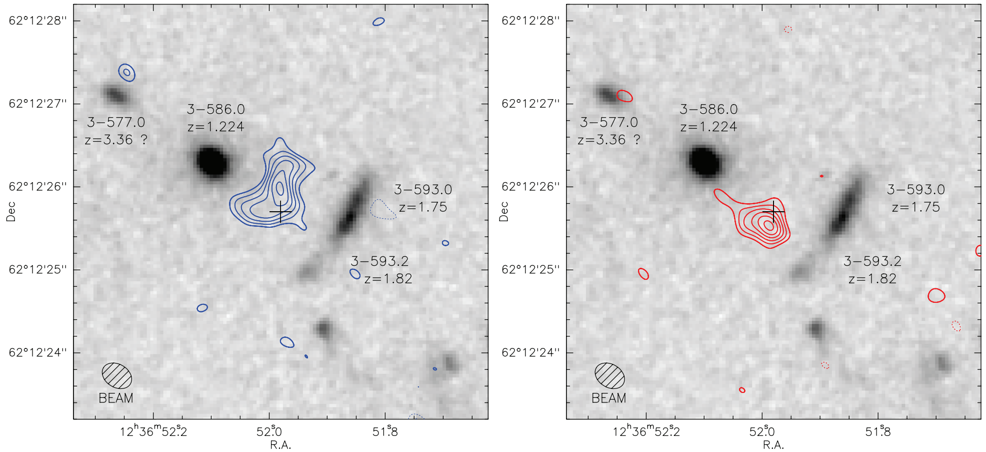

- No optical counterpart
  $\Rightarrow$ only known SMG at $z = 5.2$.
- Dust at 158 μm nearly optically thick.
- The two Gaussian component in velocity are distincts 1-2 kpc objects separated by 2 kpc.
- $L'(C^+) \sim L(CO1-0) \Rightarrow$ Starburst.

Science with IRAM-NOEMA

Topics

- Star formation throughout the history of the universe.
- Galaxy formation and evolution.
- Interstellar chemistry, star and planet formation and the potential impact on the emergence of life.
- Stellar death.
- Study of solar system.

Political aspects

- Enable large, statistically significant surveys.
- Provide easy and flexible access to discovery space.
- Generate full sky coverage in the millimeter range.
- Enhance IRAM patners use of ALMA.